OPTIMIZATION OF THE PHOTOREFRACTIVITY IN II-IV SEMICONDUCTORS

Brimrose Corporation of America

G.V. Jagannathan, S.B. Trivedi, and S.W. Kutcher

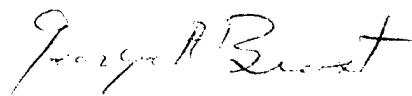*APPROVED FOR PUBLIC RELEASE; DISTRIBUTION UNLIMITED.*

19981210 030

**AIR FORCE RESEARCH LABORATORY
SENSORS DIRECTORATE
ROME RESEARCH SITE
ROME, NEW YORK**

DTIC QUALITY INSPECTED 4

This report has been reviewed by the Air Force Research Laboratory, Information Directorate, Public Affairs Office (IFOIPA) and is releasable to the National Technical Information Service (NTIS). At NTIS it will be releasable to the general public, including foreign nations.
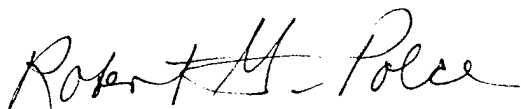
AFRL-SN-RS-TR-1998-203 has been reviewed and is approved for publication.

APPROVED:

GEORGE A. BROST
Project Engineer

FOR THE DIRECTOR:

ROBERT G. POLCE, Acting Chief
Rome Operations Office
Sesnors Directorate

If your address has changed or if you wish to be removed from the Air Force Research Laboratory Rome Research Site mailing list, or if the addressee is no longer employed by your organization, please notify AFRL/SNDR, 25 Electronic, Rome, NY 13441-4515. This will assist us in maintaining a current mailing list.

Do not return copies of this report unless contractual obligations or notices on a specific document require that it be returned.

REPORT DOCUMENTATION PAGE

Public reporting burden for this collection of information is estimated to average 1 hour per response, including the time for reviewing instructions, searching existing data sources, gathering and maintaining the data needed, and completing and reviewing the collection of information. Send comments regarding this burden estimate or any other aspect of this collection of information, including suggestions for reducing this burden, to Washington Headquarters Services, Directorate for Information Operations and Reports, 1215 Jefferson Davis Highway, Suite 1204, Arlington, VA 22202-4302, and to the Office of Management and Budget, Paperwork Reduction Project (0704-0188), Washington, DC 20503.

1. AGENCY USE ONLY *(Leave blank)*	2. REPORT DATE	3. REPORT TYPE AND DATES COVERED
	November 1998	Final Mar 96 - Mar 97

4. TITLE AND SUBTITLE
OPTIMIZATION OF THE PHOTOREFRACTIVITY IN II-IV SEMICONDUCTORS

5. FUNDING NUMBERS
C - F30602-96-C-0043
PE - 62702F
PR - 4600
TA - P2
WU - PZ

6. AUTHOR(S)
G.V. Jagannathan, S.B. Trivedi, S.W. Kutcher

7. PERFORMING ORGANIZATION NAME(S) AND ADDRESS(ES)
Brimrose Corporation of America
5024 Campbell Blvd Ste E
Baltimore MD 21236

8. PERFORMING ORGANIZATION REPORT NUMBER
N/A

9. SPONSORING/MONITORING AGENCY NAME(S) AND ADDRESS(ES)
Air Force Research Laboratory/SNDR
25 Electronic Pky
Rome NY 13441-4515

10. SPONSORING/MONITORING AGENCY REPORT NUMBER
AFRL-SN-RS-TR-1998-203

11. SUPPLEMENTARY NOTES
Project Engineer: Dr. George A. Brost, AFRL/SNDR, (315) 330-7669

12a. DISTRIBUTION AVAILABILITY STATEMENT

APPROVED FOR PUBLIC RELEASE: DISTRIBUTION UNLIMITED

12b. DISTRIBUTION CODE

13. ABSTRACT *(Maximum 200 words)*
This work was aimed at optimization of the photorefractivity in the II-VI semiconductors CdTe, ZnTe and $Cd_{x-1}Zn_xTe$ for real-time optical signal processing applications at near infrared wavelengths. During this work, several crystals of ZnTe, CdTe and $Cd_{x-1}Zn_xTe$ were grown. Crystal growth of ZnTe and CdTe was carried out using low supersaturation nucleation and "contactless" growth by Vertical Physical Vapor Transport (PVT) in closed ampoules and the CdTe and $Cd_{x-1}Zn_xTe$ crystals were grown using the vertical Bridgman technique. The quality of the crystals grown during this work was evaluated based on optical, electrical and structural characterization. Infrared microscopy was used to examine the internal crystalline structure of the samples. Most of the crystals grown during this work exhibited photorefractivity and photoconductivity. The resistivity of the vanadium doped crystals under dark conditions was found to be between 10^8 to 10^{10} Ω-cm. The resistivity decreased significantly in the presence of illumination indicating that the crystals were highly photoconductive. The photorefractive properties of the crystals grown during this project were characterized by two beam coupling. All of the measurements revealed a strong photorefractive nonlinear effect.

14. SUBJECT TERMS
II-VI Semiconductors, CdTe, ZnTe, $Cd_{x-1}Zn_xTe$, Real-Time Optical Signal Processing, Low Supersaturation Nucleation, "contactless", Vertical Physical Vapor Transport

15. NUMBER OF PAGES
40

16. PRICE CODE

17. SECURITY CLASSIFICATION OF REPORT	18. SECURITY CLASSIFICATION OF THIS PAGE	19. SECURITY CLASSIFICATION OF ABSTRACT	20. LIMITATION OF ABSTRACT
UNCLASSIFIED	UNCLASSIFIED	UNCLASSIFIED	UL

ACKNOWLEDGMENTS

TABLE OF CONTENTS

LIST OF FIGURES

1.0   Executive Summary

The proposed work was aimed at optimization of the photorefractivity in the II-VI semiconductors CdTe, ZnTe and $Cd_{1-x}Zn_xTe$ for real-time optical signal processing applications at near infrared wavelengths. Our goal was to obtain application quality photorefractive crystals with a minimal concentration of intrinsic and extrinsic point defects, dislocation density and twins in these crystals. We were able to achieve these goals though the following material processing steps: extensive purification of the starting materials, purification of the compounds, crystal growth under controlled conditions of heat and mass transfer, in situ annealing of the crystals subsequent to growth and annealing of the crystalline samples under various partial pressures of cadmium and tellurium vapors. Optimization of the temperature distribution in the melt and a careful control of the solid/liquid interface was used to minimize stress, the density of dislocations and the concentration of twins in the resulting crystals. Post-growth annealing in the presence of cadmium/tellurium vapor was performed to lower the dislocation density, the vacancy concentration and the concentration of tellurium precipitates.

During this work, several crystals of ZnTe, CdTe and $Cd_{1-x}Zn_xTe$ were grown. The crystals were doped with either vanadium or both vanadium and manganese. We found during our work that only the transition metal vanadium was successful in producing photorefractivity when used as the dopant in the CdTe and $Cd_{1-x}Zn_xTe$ crystals. The addition of manganese along with the vanadium was found to enhance the photorefractive properties of the crystals, but manganese alone did not induce photorefractivity in the crystals. We also found that the transition metal scandium produced photorefractive material when added to ZnTe, so during this project, one scandium doped ZnTe crystal was grown. At this time, the role of the vandium dopant in the band structure of the photorefractive crystals is not clearly understood. Thus, further study into this area is needed in order to optimize the photorefractive gain of these crystals.

Crystal growth of ZnTe and CdTe was carried out using low supersaturation nucleation and "contactless" growth by vertical physical vapor transport (PVT) in closed ampoules [6,7]. The growth rate as a function of furnace profile, ampoule geometry, material stoichiometry and hydrogen pressure was investigated. We determined a method to improve stoichiometry of the source material during crystal growth by lowering the partial pressure of the excessive component to levels that were controlled by the temperature of the cold zone, pulling rate of the ampoule and crystal growth rate. Our investigation of temperatures suitable for nucleation and "contactless"

1

growth also led to optimal conditions for stability of the growth interface. We determined a constitutional supersaturation criterion which ensures a stable growth interface. Additionally, CdTe and $Cd_{1-x}Zn_xTe$ crystals were grown using the vertical Bridgman technique.

The quality of the crystals grown during this work was evaluated based on optical, electrical and structural characterization. Infrared microscopy was used to examine the internal crystalline structure of the samples. Most of the crystals grown during this work exhibited photorefractivity and photoconductivity. The resistivity of the vanadium doped crystals under dark conditions was found to be between 10^8 to 10^{10} Ω-cm. The resistivity decreased significantly in the presence of illumination indicating that the crystals were highly photoconductive. The absorption spectrum from the ZnTe and CdTe samples generally showed fairly low absorption in the near infrared wavelength range. However, it is difficult to obtain high quality $Cd_{1-x}Zn_xTe$ with low absorption because of the separation between the liquidus and solidus curves in the pseudobinary phase diagram of CdTe-ZnTe [13]. Thus, we were only able to obtain one crystal of $Cd_{1-x}Zn_xTe$ with acceptable transmission. This crystal did exhibit photorefractivity with a gain of ~ 0.27 cm^{-1} at a wavelength of 1.3 μm and at a grating spacing of 1 μm.

The photorefractive properties of the CdTe and ZnTe crystals grown during this project were characterized by two beam coupling. The measurements were carried out at 0.633μm, the semiconductor laser wavelength range of 0.700 to 0.850μm, and the important optical communication wavelengths of 1.3 and 1.5μm. All of the measurements revealed a strong photorefractive nonlinear effect. In vanadium doped ZnTe, we observed a photorefractive gain of 0.6cm^{-1} at a wavelength of 0.80μm and a grating spacing of 1μm. The photorefractive gain observed in vanadium-manganese codoped ZnTe was much higher than the gain in ZnTe:V. The photorefractive gain in ZnTe:V:Mn (at 1μm grating spacing) at 0.63μm was 1.52cm^{-1} and at 0.80μm it was 1.3cm^{-1}. In CdTe:V, the two beam coupling gain at $\Lambda_g = 0.6\mu$m and $\lambda = 870$nm was approximately 1.1 to 1.2 cm^{-1}.

2.0   Introduction

A current need exists for photorefractive materials operating at near infrared wavelengths for real-time optical processing applications at room temperature. Brimrose has been a leading company internationally and perhaps the only company in the country .to have produced photorefractive semiconductors such as CdTe:V [1,2], ZnTe:V [3,4] and $Cd_{1-x}Zn_xTe$:V [4] which operate at near infrared wavelengths. However, the factors affecting the reproducibility, uniformity of photorefractive response and mobility-lifetime product are not completely understood. Furthermore, the relation between the photorefractive response and the nature and concentration of the dopant/s is not fully understood.

Efficient photoconductivity is a prerequisite for the photorefractive process and affects the saturation intensity, the efficiency and the speed of non-linearity. Also, the ability to write an efficient grating at low intensity levels requires a large dark resistivity. Both the resistivity and photoconductivity of any photorefractive material depends on its transport properties, carrier mobility and lifetime. In an ideal undoped crystal at a given temperature, mobility is a material

property that depends on the effective carrier mass and optical phonon structure. However, to induce photorefractivity in II-VI compound semiconductors, doping with transition element impurity/impurities having levels deep within the energy bandgap of the host material is required. For extrinsically and intrinsically doped "non-ideal" crystals, the mobility and the lifetime depend upon the physical and chemical imperfections in the crystal (dislocation density, twinning, and other recombination centers in the crystal lattice). Thus, a reduction in these imperfections can improve the crystal's transport properties.

It is evident in our previous work [1-5], that the optimization of the photorefractive effect in II-VI semiconductors is largely dependent on the type of dopant and the nature of the host matrix. Electron-paramagnetic resonance (EPR) studies clearly revealed that the vanadium levels are optically active in CdTe:V. However, in similar studies of ZnTe:V, the signature of vanadium incorporation in the crystal lattice was not observed. Also, the photorefractive effect was more pronounced in CdTe:V compared to ZnTe:V. Furthermore, the addition of manganese to ZnTe:V enhanced the photorefractivity while the effect of manganese addition to CdTe:V was not significant. Thus, the nature and concentration of the dopant as well as the nature of the host matrix have a significant impact on the photorefractive properties of these crystals.

This work was aimed at optimizing the photorefractivity in the II-VI semiconductors CdTe, ZnTe and $Cd_{1-x}Zn_xTe$. Our goal was to obtain application quality photorefractive crystals with a minimal concentration of intrinsic and extrinsic point defects, dislocation density and twins in these crystals. This was achieved though the following material processing steps: extensive purification of the starting materials, purification of the compounds, crystal growth under controlled conditions of heat and mass transfer, insitu annealing of the crystals subsequent to growth and annealing of the crystalline samples under various partial pressures of cadmium and tellurium vapors. Optimization of the temperature distribution in the melt and a careful control of the solid/liquid interface was used to minimize stress, the density of dislocations and the concentration of twins in the resulting crystals. Post-growth annealing in the presence of cadmium/tellurium vapor was performed to lower the dislocation density, the vacancy concentration and the concentration of tellurium precipitates.

The quality of the crystals was evaluated based on optical, electrical and structural characterization. The photorefractive measurements conducted during this work were carried out at $0.633\mu m$, the semiconductor laser wavelength range of 0.700 to $0.850\mu m$, and the important optical communication wavelengths of 1.3 and $1.5\mu m$. With the successful growth of high quality crystals, our materials can be used in various applications involving detectors and electro-optic devices.

3

3.0 Crystal Growth

3.1 Purification

Both intrinsic and extrinsic defects affect the optoelectronic properties of ZnTe, CdTe, and $Cd_{1-x}Zn_xTe$. In order to improve the producibility of high quality crystals, extensive purification of the constituent elements, cadmium, tellurium and zinc, was carried out. The received elements were 99.9999% pure. These elements have relatively low melting points (T_m(cadmium)=320°C, T_m(zinc)=420°C and T_m(tellurium)=450°C), and relatively high vapor pressures at low temperatures. Therefore, both sublimation and distillation under dynamic vacuum ($\approx 10^{-6}$ torr) were used for further purification. In order to prevent the transfer of the non-volatile or less volatile impurities in the condensation region, sublimation of these materials was not carried out to completion.

3.2 Low Supersaturation Nucleation and "Contactless" Growth

Crystal growth of ZnTe and CdTe was carried out using low supersaturation nucleation and "contactless" growth by vertical physical vapor transport (PVT) in closed ampoules [6-8]. This method is described as follows.

Source material was vacuum sealed in fused silica ampoules that were about 20cm long with an inner diameter of 25mm. An inert atmosphere of approximately 50mbar of high purity hydrogen was created in the ampoule prior to sealing. The ampoule consisted of three chambers separated by two plugs. The diameter of these plugs was slightly smaller than the inner diameter of the ampoule. The plug located between the second and third zones was sealed to the ampoule wall such that only a narrow slit was left unsealed, making possible the slow transport of gases between zones II and III. The plug located between the first and second zones was fixed to the ampoule wall, but the slit between the plug and the ampoule wall was mostly unsealed.

Prior to growth, the source material was placed in zone II. The ampoule was placed in a furnace with a sharp parabola-like temperature profile such that zone II was located at the maximum temperature (1050°C), zone I was located at a temperature approximately 50°C lower, and zone III at a temperature 400°C lower. Such a configuration allowed the transport of gases from zone II to both zones I and III. However, the difference in cross section of the slits between the plugs and ampoule wall, as well as the difference in temperature between the zones, caused a majority of the source material to be transported to zone I, and deposition of the excessive component in zone III.

After the source material was fully transported from zone II, the ampoule was shifted such that the material was transported from zone I back into zone II. Since the temperature of the plug between zones I and II was only a few degrees lower than the surface of the source material, spontaneous nucleation did not occur on the front of the plug. Both axial and radial temperature

4

gradients across the source material caused a change in the shape of its surface such that a cone with a monocrystalline peak aimed at the plug was formed. A further increase in the temperature gradient between the source material and the plug separating zones I and II (also called the crystal holder) led to adhesion of the monocrystalline part of the source to the crystal holder, separation from the source material, and growth of the ZnTe or CdTe crystal by PVT. Figure 1a through 1g show the stages of low supersaturation nucleation and "contactless" growth of a crystal. A photograph of a ZnTe crystal still attached to the crystal holder is shown in Figure 2.
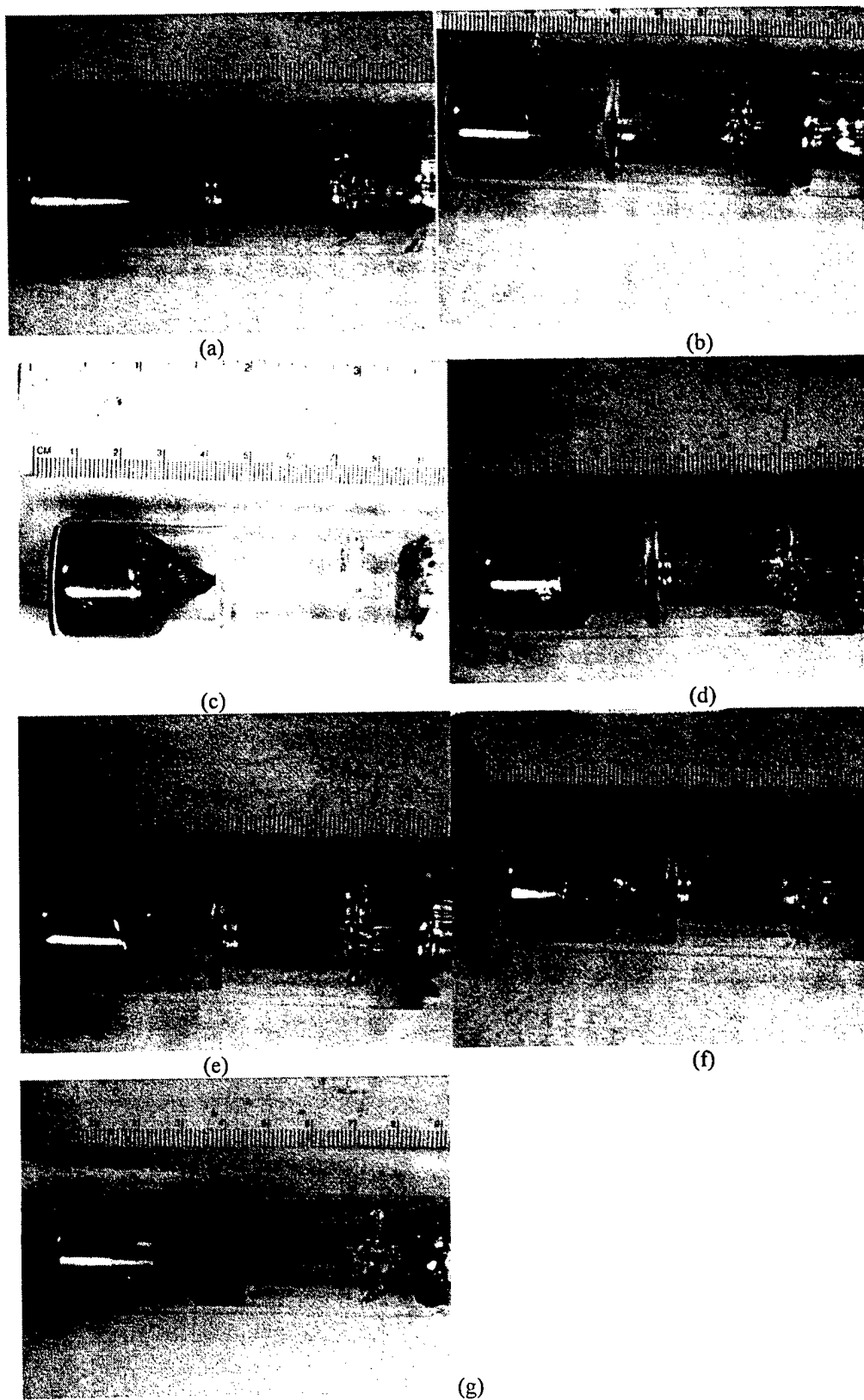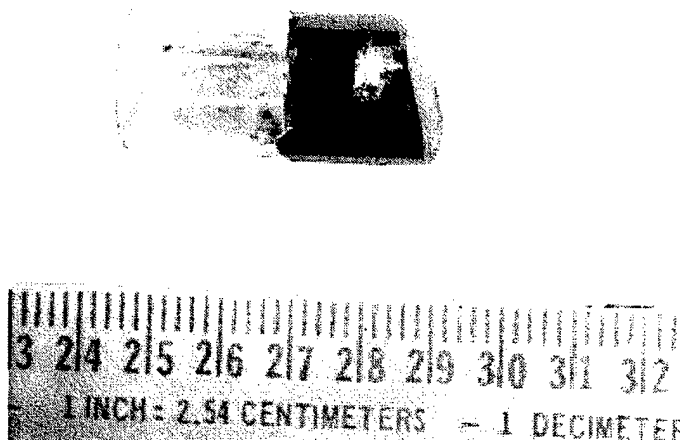
Figure 1. Stages of low supersaturation nucleation and "contactless" growth.

Figure 2   ZnTe crystal still attached to the crystal holder.

The growth rate as a function of furnace profile, ampoule geometry, material stoichiometry and hydrogen pressure was investigated. The maximum furnace temperature was in the range of 815-1050°C. We were looking for optimal conditions for the highest growth rate at the lowest possible temperature. The highest transport rate (a few mm/day at 815°C and a temperature gradient of 10°C/cm) was obtained in an ampoule where carefully prepared near stoichiometric material was sealed under high vacuum (10^{-6} torr) without hydrogen. However, at such a low temperature the crystal was not single. Additionally, under these growth conditions, most of the material was transported to zone II and the size of the crystal was relatively small. Using the ampoule described above, material containing an excess of tellurium, a growth temperature of 1050°C and a growth rate in the range of 5-10mm/day, good reproducibility of the growth conditions was achieved. Growth of "contactless" crystals at this high temperature (1050°C) decreases the risk of constitutional supersaturation instabilities. However, the fast transport rate must be limited by an excess component in the vapor phase such as tellurium or an inert gas.

The growth of ZnTe and CdTe crystals by PVT from near stoichiometric source material is possible over a relatively wide range of temperatures due to its high saturated vapor pressure at temperatures far below the melting point [9]. However, it is extremely difficult to control the transport rates in nearly stoichiometric material. If the *in situ* purified material is removed from the ampoule and mechanically crushed and powdered, its surface oxidizes relatively fast in the presence of air, and the material is apt to lose its stoichiometry during sealing of the growth ampoule. If compacted, the material stoichiometry is generally poor and hard to improve.

The method of improving stoichiometry of the source material during crystal growth used here satisfactorily stabilizes the growth conditions by lowering the partial pressure of the excessive component to levels controlled by the temperature of the cold zone, pulling rate of the ampoule and

7

crystal growth rate. The procedure of pre-subliming the material from zone II to zone I considerably improves the uniformity of distribution of the transition metal dopants. It is transported from the non-compacted source through the slit in amounts adequate to impose transport conditions. The excess of non-volatile transition metal elements stays in zone II and does not disturb further growth of the crystal. Also, the eventual non-volatile impurities of the source material stay in zone II and cannot be transported to zone I by convection.

The method of low supersaturation nucleation ensures formation of good quality seeds. The investigation of temperatures suitable for nucleation and "contactless" growth also leads to optimal conditions for stability of the growth interface. According to our constitutional supersaturation criterion [10,12], the stable growth interface results from a low ratio of the gradient of vapor above the interface and the gradient of temperature along the crystal close to the interface. Thus, more stable growth is always expected for low growth rates. An increase in the growth rate with a stable interface is possible only at higher temperatures [11,12] or steeper furnace temperature gradients. However, an increase in temperature as well as an increase in the furnace temperature gradient is limited by temperature-dependent thermal properties of the growing material.

3.3   Bridgman Growth

Crystal growth of CdTe and $Cd_{1-x}Zn_xTe$ was carried out using the vertical Bridgman technique. For synthesis, the purified starting materials were carefully weighed in correct stoichiometric proportions and placed in graphitized fused silica ampoules (approximately 20cm long and 20mm in diameter). Vanadium was added so that the starting concentration of the dopant was $1x10^{19}$ atoms/cm^3. After being vacuum sealed, the ampoules were placed in a three zone Bridgman furnace. The temperature of the furnace was controlled as follows: 1) increased to 600°C in two hours and held constant for 12 hours; 2) increased to 1125°C over 24 hours; 3) held constant and allowed to react and mix for 24 hours; 4) decreased to room temperature over a 24 hour period.

The synthesized ingots were removed and cleaned in a bromine in methanol solution and resealed under vacuum in graphitized fused silica ampoules. The individual ampoules were again placed in the Bridgman furnace and the temperature was increased to 1125°C in 24 hours. The material was kept in the molten state for approximately 24 hours. Crystal growth was started by translating the ampoule down across the temperature gradient. The lowering rate was 2mm/hour and the temperature gradient was 20°C/cm (4°C/hour). After solidification was complete, the boule was kept at a temperature between 925 and 975°C and allowed to anneal for a period of 48 hours. Finally, the furnace was brought to room temperature at a rate of about 1°C/min.

3.4   Sample Preparation

During this work, several crystals of ZnTe, CdTe and $Cd_{1-x}Zn_xTe$ were grown. The crystals were doped with either vanadium or both vanadium and manganese. One ZnTe crystal that was grown was doped with scandium (ZnTe:Sc). An example of wafer-like pieces that were cut from a single crystalline section of a CdTe:V boule are shown in Figure 3.

8
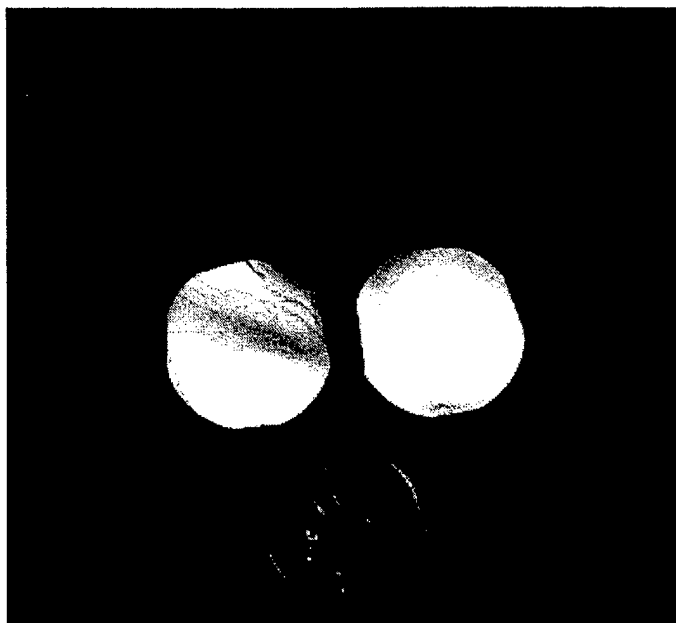
Figure 3   Wafer-like pieces that were cut from a single crystalline section of a CdTe:V boule.

The cleavage planes are clearly seen in these photos. A section of the vanadium-manganese co-doped ZnTe crystal is shown in Figure 4(a) and Figure 4(b). The first grown part of the crystal, grown close to the crystal holder, is characterized by a strong tendency to twinning. Additionally, adhesion of the crystal to the crystal holder resulted in cracking of this part of the crystal. The last grown part of the crystal, located far from the crystal holder, showed less twinning behavior. Traces of cracking were not found in this part of the crystal. We also grew a large 77 gram boule of ZnTe:V during this work. A photograph of a section of this crystal is shown in Figure 5. It was mostly single crystalline with small grains on the outer edges.
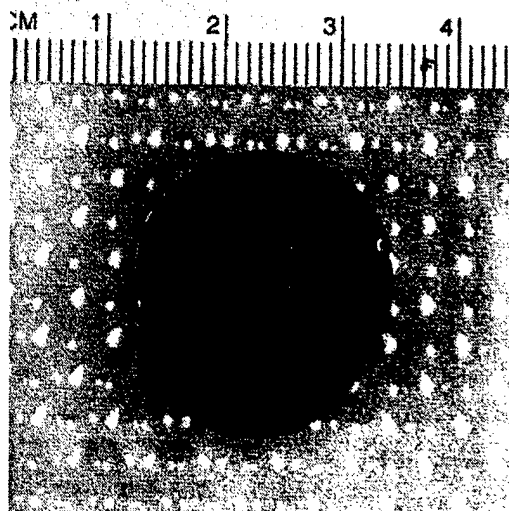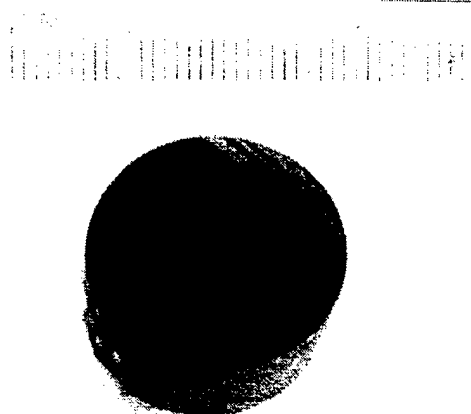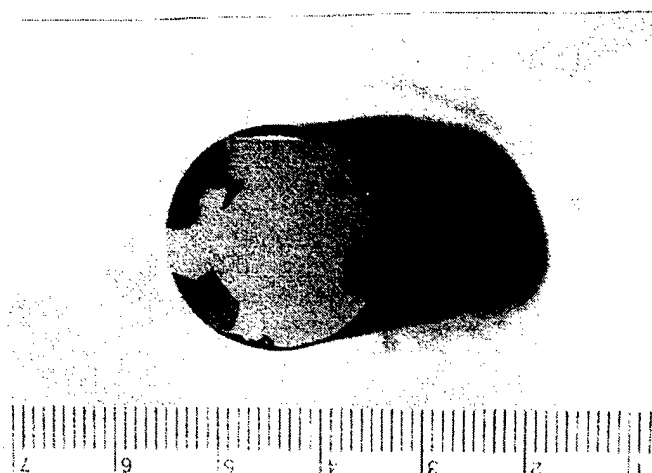
<center>(a)   (b)</center>

**Figure 4 a & b   Section of co-doped ZnTe:V:Mn crystal.**

Figure 5   Section of 77 gram ZnTe:V crystal.

The crystals were oriented using x-ray diffraction. An example of a Laue pattern from a CdTe:V crystal is shown in Figure 6, and the Laue photographs of a ZnTe:V sample and a ZnTe:Mn:V sample are shown in Figure 7. The size and shape of the Laue spots are indicative of good quality crystals. Samples were cut and mechanically lapped and polished. The samples had an orientation of <110>x<110>x<100>.The individual crystal samples were then used for further analysis.

<center>10</center>
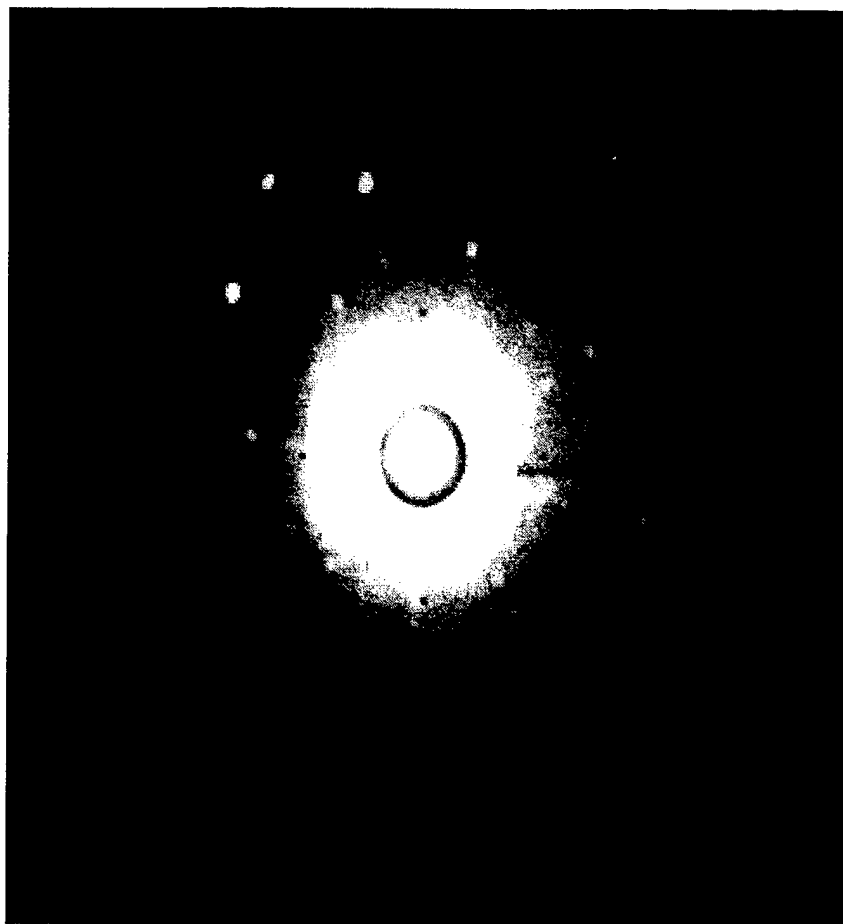
Figure 6   **Laue pattern from a CdTe:V crystal.**
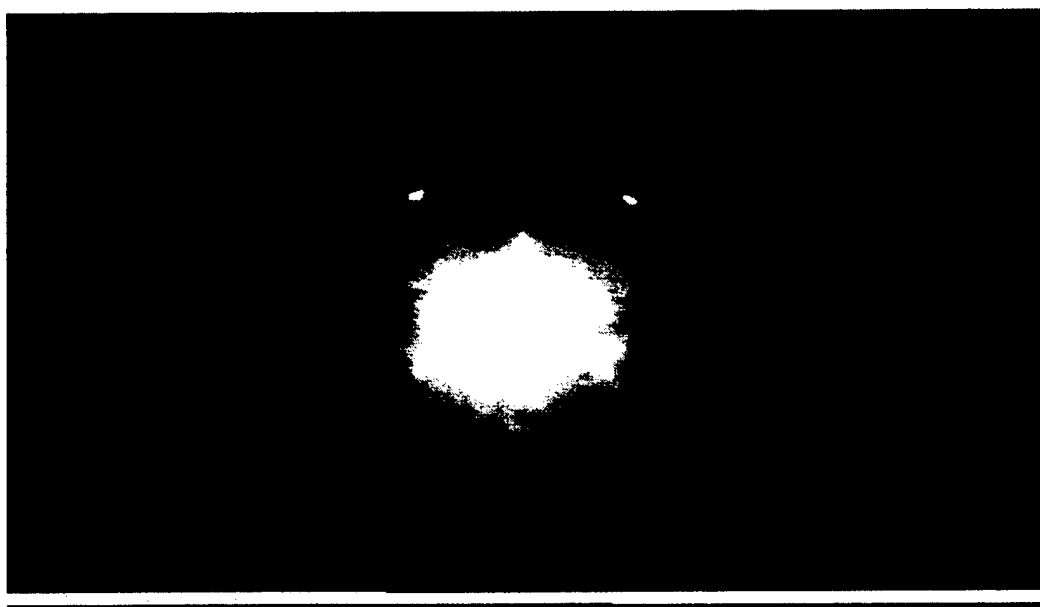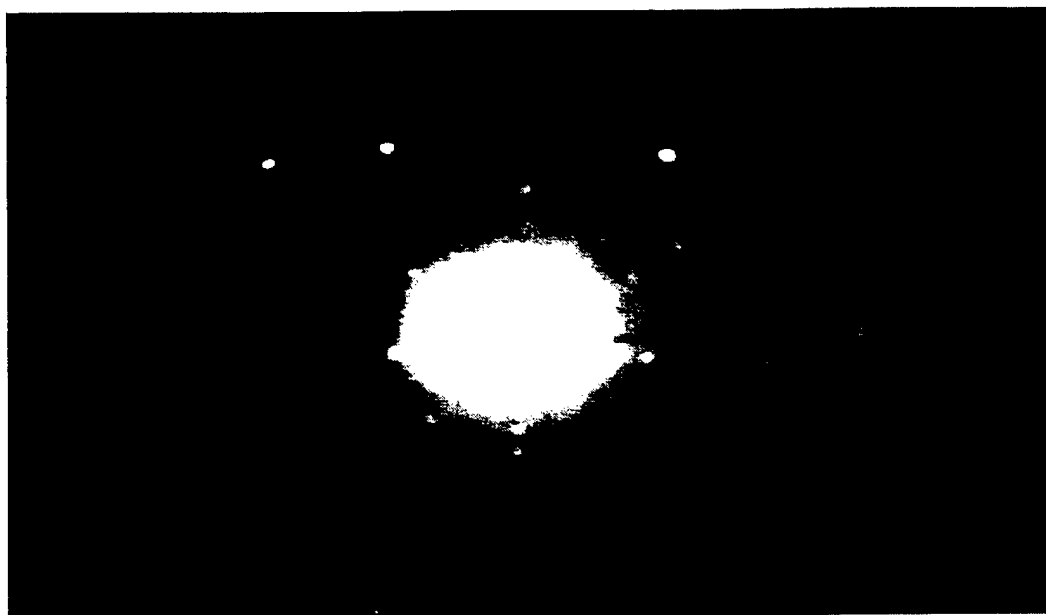
Figure 7   Laue photographs of the (110) face of ZnTe:V (top) and ZnTe:Mn:V (bottom).

4.0 Crystal Characterization

4.1 Characterization of CdTe

Infrared microscopy was used for examination of the crystalline structure of the CdTe:V samples. With an infrared microscope we were able to view the surface and the bulk of the crystals. Pictures taken within the bulk material of a CdTe:V crystal are shown in Figure 8. These photos show the presence of precipitates and inclusions within the bulk of the crystal. (The scratch-like marks in the photo on the right are surface marks that had carried through into the bulk). For comparison purposes, we also examined a CdTe substrate that we obtained from a commercial supplier. Pictures taken using the IR microscope of the bulk of this sample clearly show the presence of a fairly high concentration of precipitates. The pictures are also very "foggy" in appearance indicating lower crystalline quality compared to CdTe crystals grown at Brimrose during this project.

The CdTe:V crystals grown during this work exhibited photorefractivity and photoconductivity. The resistivity of the CdTe:V crystals under dark conditions were found to be between 10^8 to 10^{10} Ω-cm. The resistivity decreased significantly in the presence of illumination indicating that the crystals were highly photoconductive. The absorption coefficient of the CdTe:V crystals were typically between 3 and 4 cm^{-1} over the wavelength range of interest. Plots of transmission and absorption coefficient versus wavelength for a CdTe:V crystal are shown in Figure 9. The two beam coupling gain coefficient as a function of grating spacing for a CdTe:V crystal is shown in Figure 10. The peak two beam coupling gain was approximately 0.8 cm^{-1} at $\Lambda_g = 0.6$ μm.
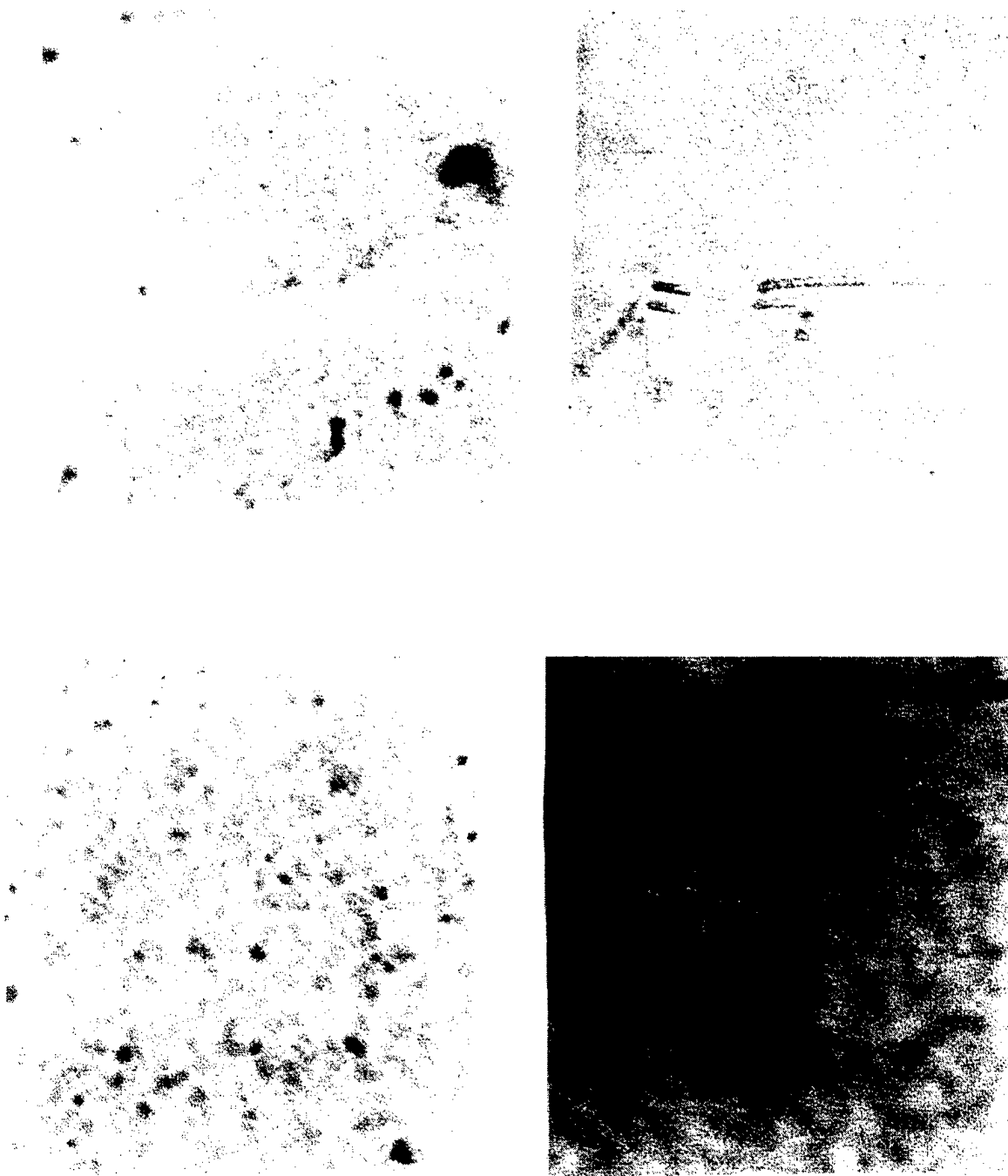
Figure 8   **Infrared microscopic photos of CdTe:V crystals**
Scale (left) = 100 μm/inch (right) = 50 μm/inch.
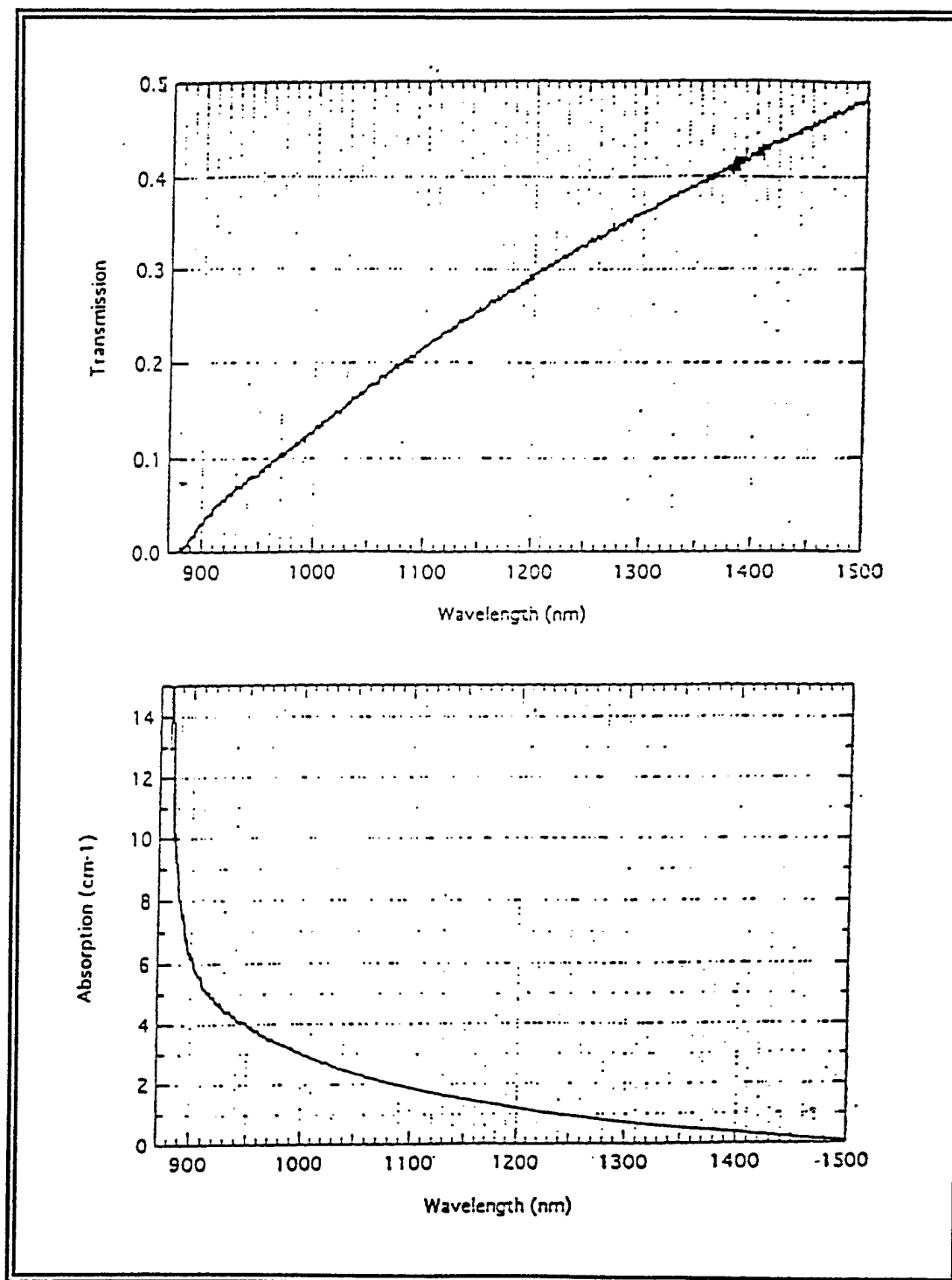
Figure 9 Transmission and absorption versus wavelength for CdTe:V.
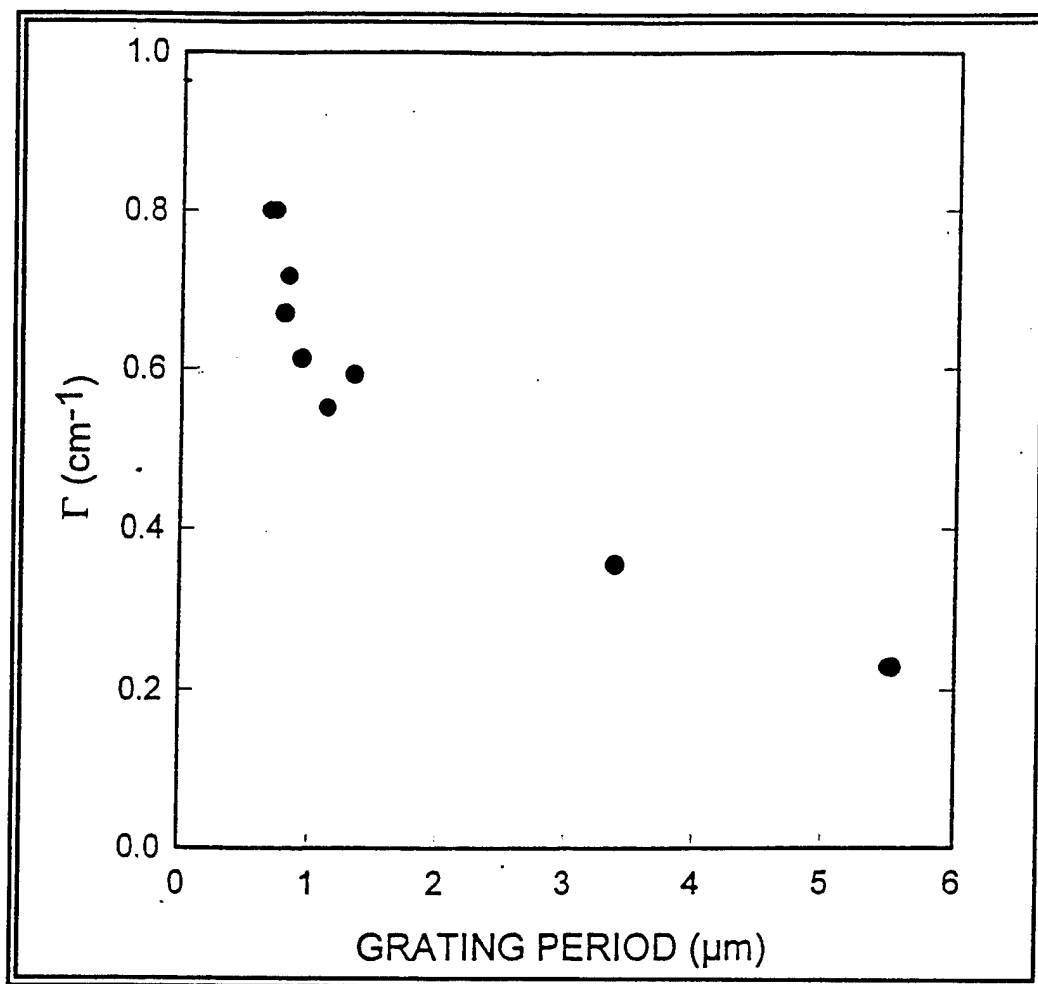
Figure 10   Two beam coupling gain versus grating period for CdTe:V.

A co-doped sample of CdTe (CdTe:V:Mn) was analyzed using a diode pumped Cr:LiSAF laser (cw) that has a tuning range from 850nm to 925nm. The absorption coefficient as a function of wavelength (Figure 11) shows α to be on the order of 5 cm^{-1}. This high absorption coefficient was due to the high doping level in the crystal. We also found that there was no obvious intensity dependence in the absorption (Figure 12) indicating that there is most likely only one set of photorefractive centers. The two beam coupling gain coefficient as a function of grating spacing at 870 nm is shown in Figure 13. The pump beam intensity was approximately 2 W/cm^2, and the pump to signal beam intensity ratio was $\approx$ 40:1. The two beam coupling gain was 1.1 to 1.2 cm^{-1} at $\Lambda_g = 0.6$ μm. This measurement was performed with no externally applied field. Assuming that the electro-optic coefficient does not vary much with the internal beam angle and the relative dielectric constant is approximately $\varepsilon_r \approx 10$, then the effective trap density can be calculated to be $N_{eff} \approx 1.5 \times 10^{15}$ cm^{-3}. We also measured the coupling as a function of wavelength for a fixed grating spacing (0.84μm) and beam ratio (Figure 14). This plot shows that once the wavelength is away from the band edge, the coupling response is fairly flat.

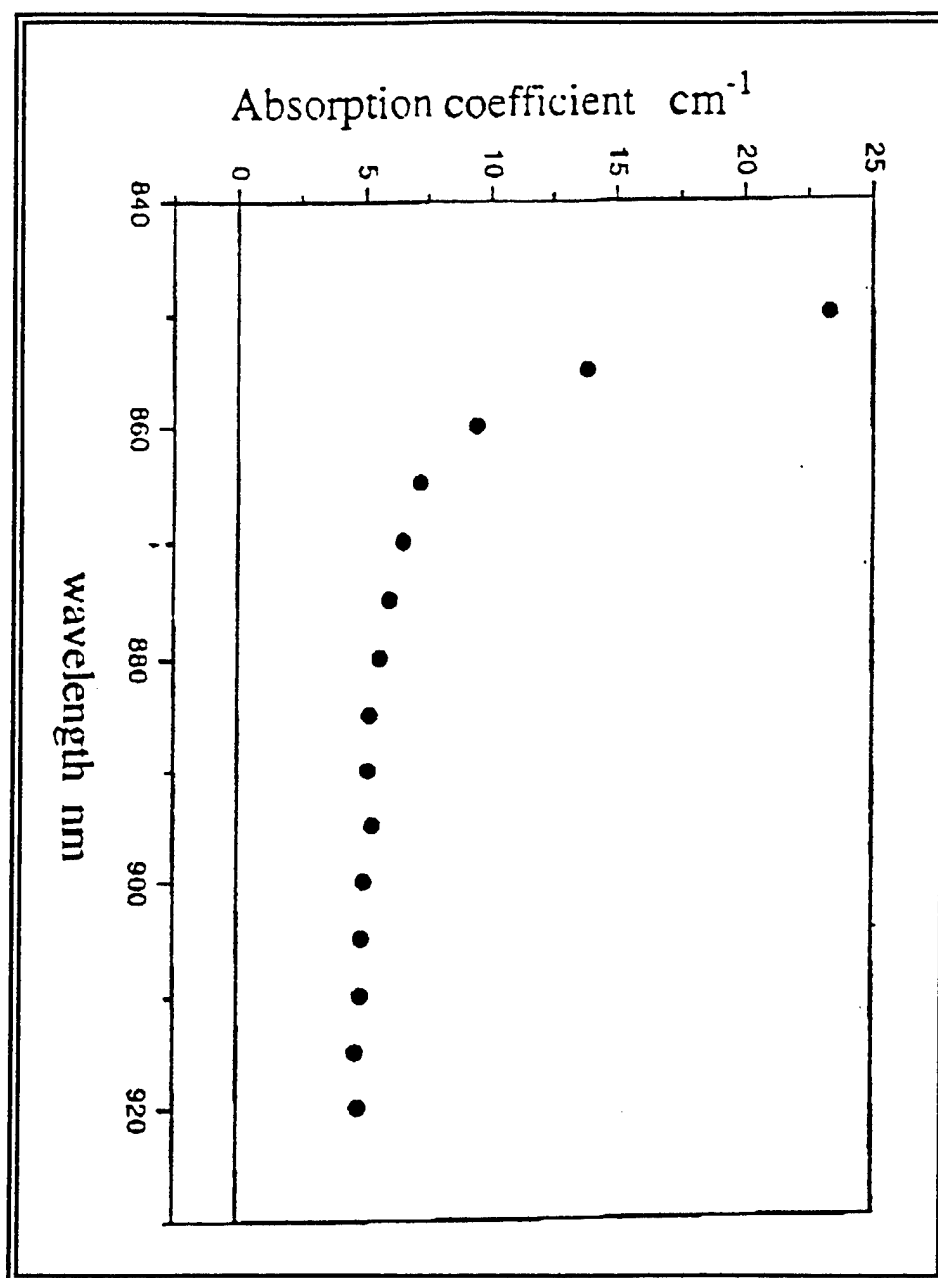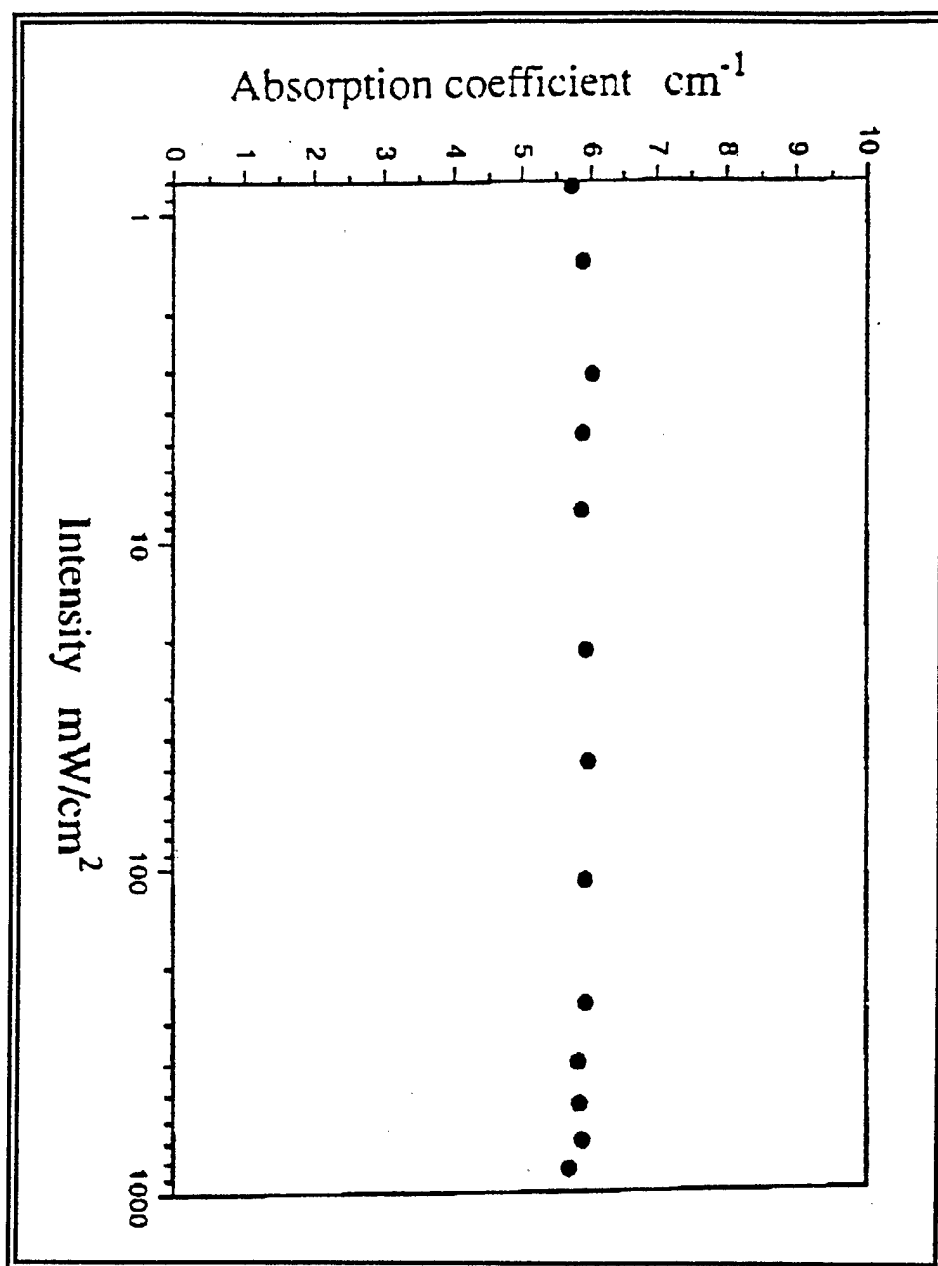**Figure 11**   Absorption coefficient versus wavelength for CdTe:V:Mn.

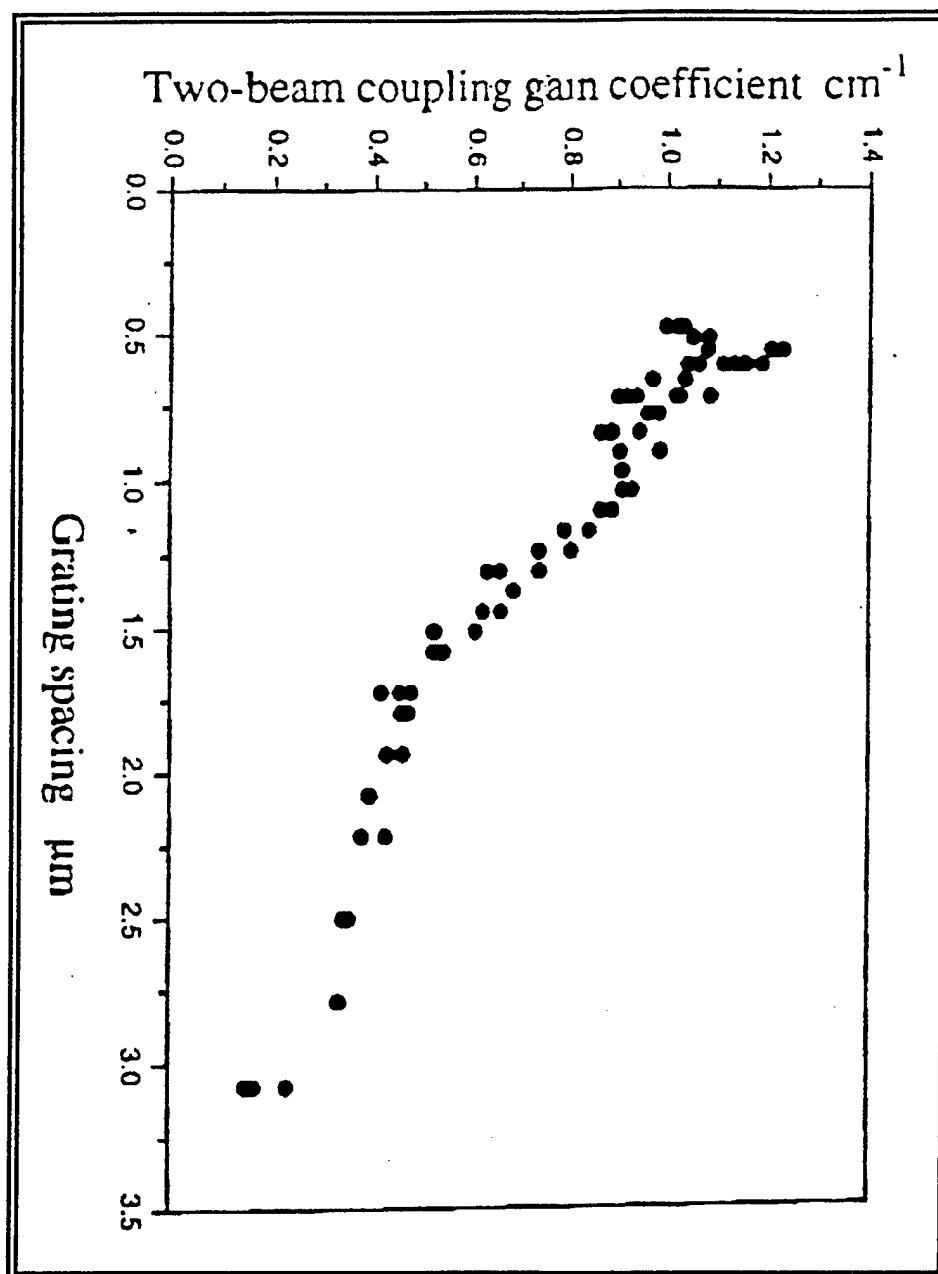**Figure 12**   Intensity dependence of absorption of CdTe:V:Mn.

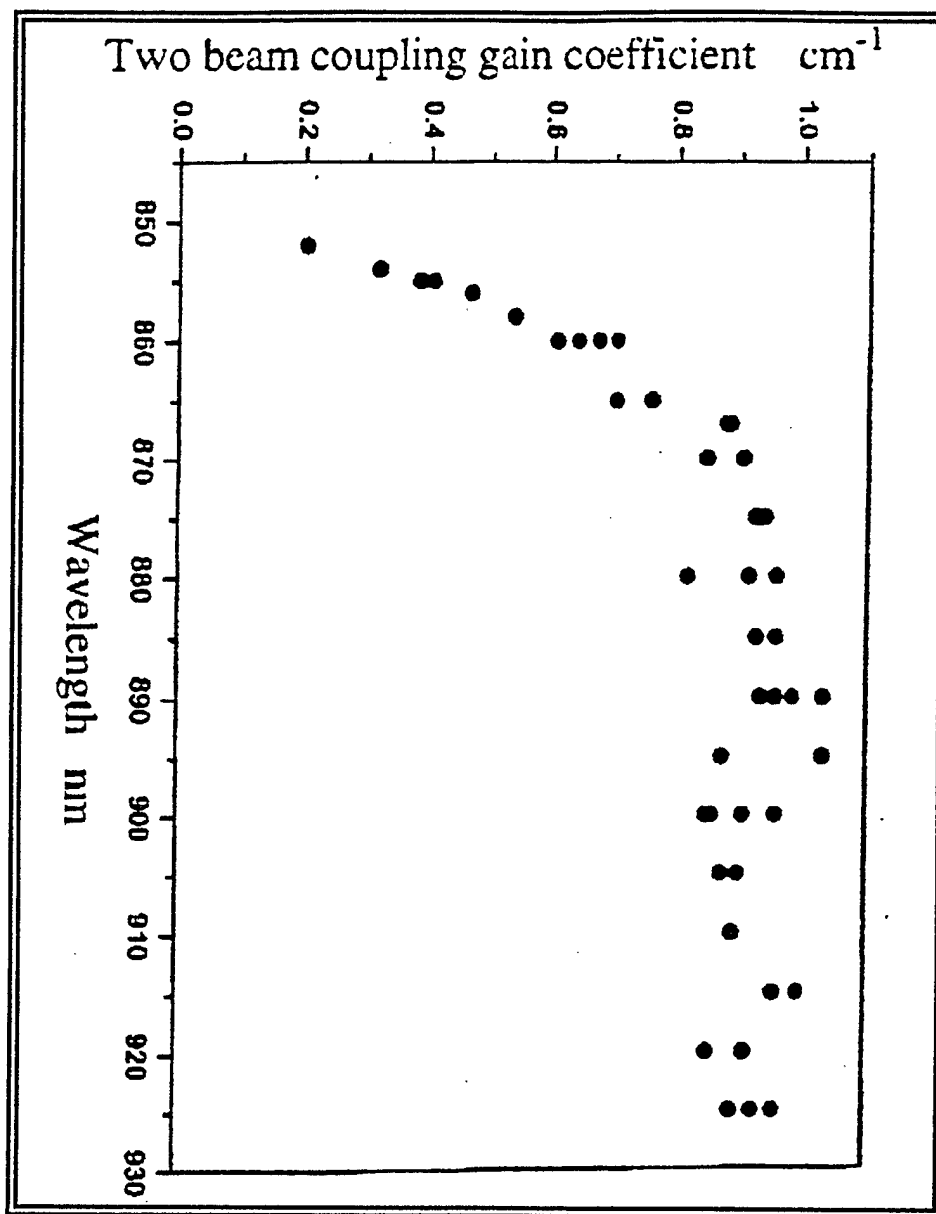**Figure 13**   Two beam coupling gain versus grating spacing at 870nm for CdTe:V:Mn.

Figure 14   Two beam coupling gain as a function of wavelength for a fixed
grating spacing of 0.84μm and fixed beam ratio for CdTe:V:Mn.

4.2   Characterization of ZnTe

Infrared microscopy was used to examine the structural properties within the bulk of several of the ZnTe crystals. The photos at the top of Figure 15 show the bulk crystalline structure at different depths within a ZnTe:V:Mn as-grown sample. These photos show the presence of precipitates and "decorated" twins (impurity defects at the location of the twin). The photos at the bottom of Figure 16 are from an annealed crystal of ZnTe:V. Precipitates can also be seen in these photos as well as cross-hatch markings, which may represent micro-twins.
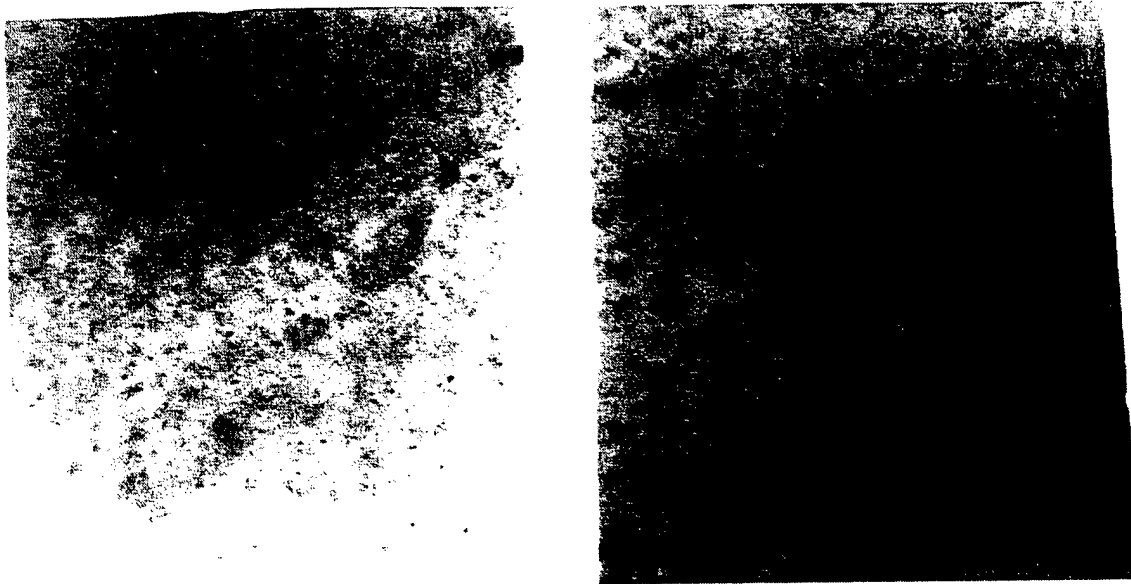
21

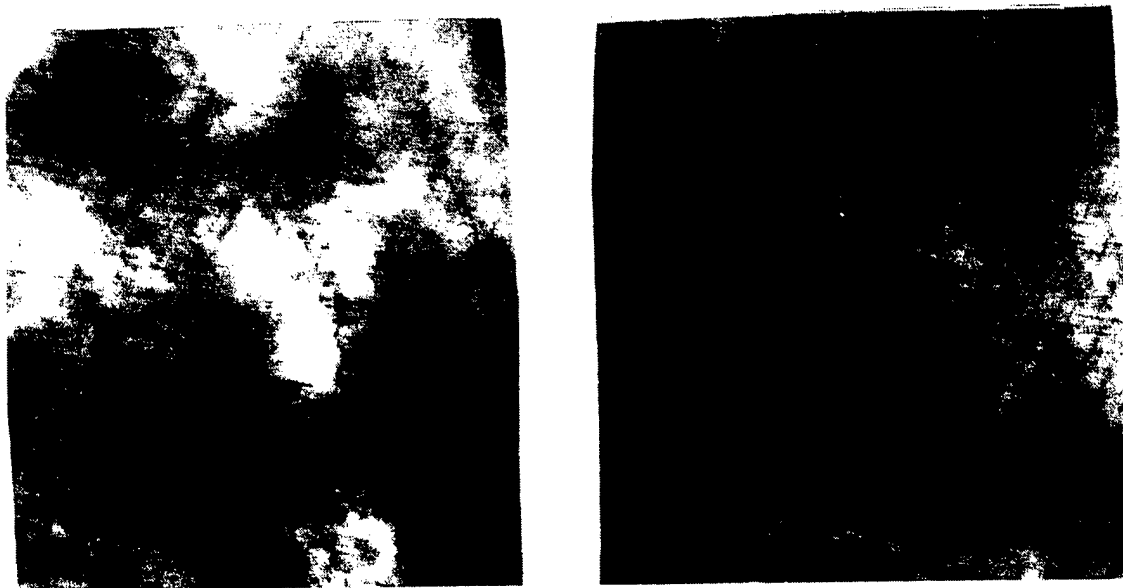Figure 15. Infrared microscope pictures of as-grown ZnTe:V:Mn (scale 100μm/inch).

Figure 16. Infrared microscope pictures of annealed ZnTe:V (scale 100μm/inch).

Figure 17 show photographs taken using the infrared microscope within the bulk of a vanadium doped sample (left) and a vanadium-manganese co-doped sample. Both of these crystals showed very uniform bulk properties with the presence of submicron precipitates. The shadings seen within these photos are characteristic of crystals which exhibit photorefractivity. Using a visible microscope, we were able to view the internal scattering of a ZnTe:V crystal. A photograph taken using this microscope is shown in Figure 18. This crystal showed significant scattering, particularly at the sights of precipitates.

For good photorefractivity, very high resistivity samples were required. The resistivity of our samples was measured using a simple circuit in which the sample was connected in series with known and thermally stable resistors. All as-grown crystals were p-type and had a very high resistivity in the range of $5x10^8$ to $1x10^{10}\Omega$-cm. A vanadium-manganese co-doped crystal had a relatively lower resistivity of 10^5 - 10^6 Ω-cm. This was to be expected since the addition of manganese to the crystal typically increases the photorefractivity but decreases the resistivity.

The nature of the spectral absorption of the sample in the vicinity of the band-edge provided the preliminary indication of the photorefractive properties of the sample. Detailed optical absorption spectroscopy was carried out in the 580 to 2000nm wavelength range for each sample. This long measurement range provided valuable information about the deep centers, native defects, shallow levels and scattering properties of the ZnTe samples. Features in the optical absorption spectra between 800 to 1600nm appear to be due to the vanadium dopant.

The photorefractive properties were characterized by two beam coupling. Two S-polarized unexpanded Gausian beams with a beam ratio of 20:1 in the <110> plane forming a grating along <001> direction was used. Measurements of photorefractive gain of a ZnTe:V crystal at 775nm, 860nm and 1064nm are shown in Figures 19 through 21, respectively. The solid curve in these figures are fit using the single carrier, single trap model. The effective carrier concentrations for each plot are shown on the figures and range from 0.8×10^{15} to 3.0×10^{15} cm^{-3}. All the measurements revealed a strong photorefractive nonlinear effect.
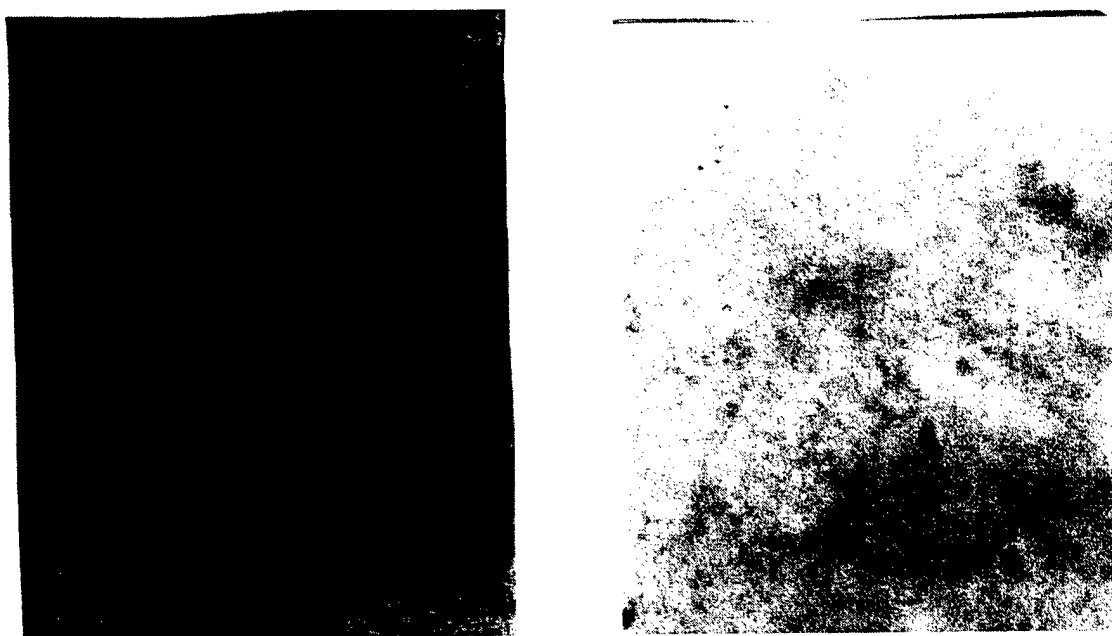
23

Figure 17. Infrared microscope pictures taken within the bulk of a ZnTe:V crystal (left) and a ZnTe:Mn:V crystal (right); scale 100μm/inch).
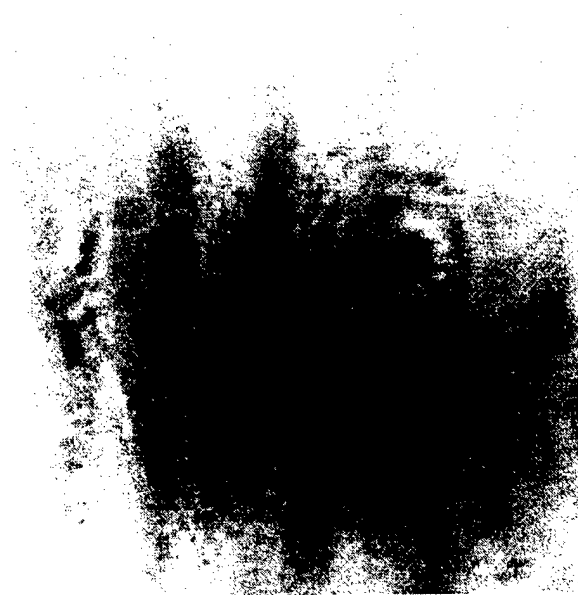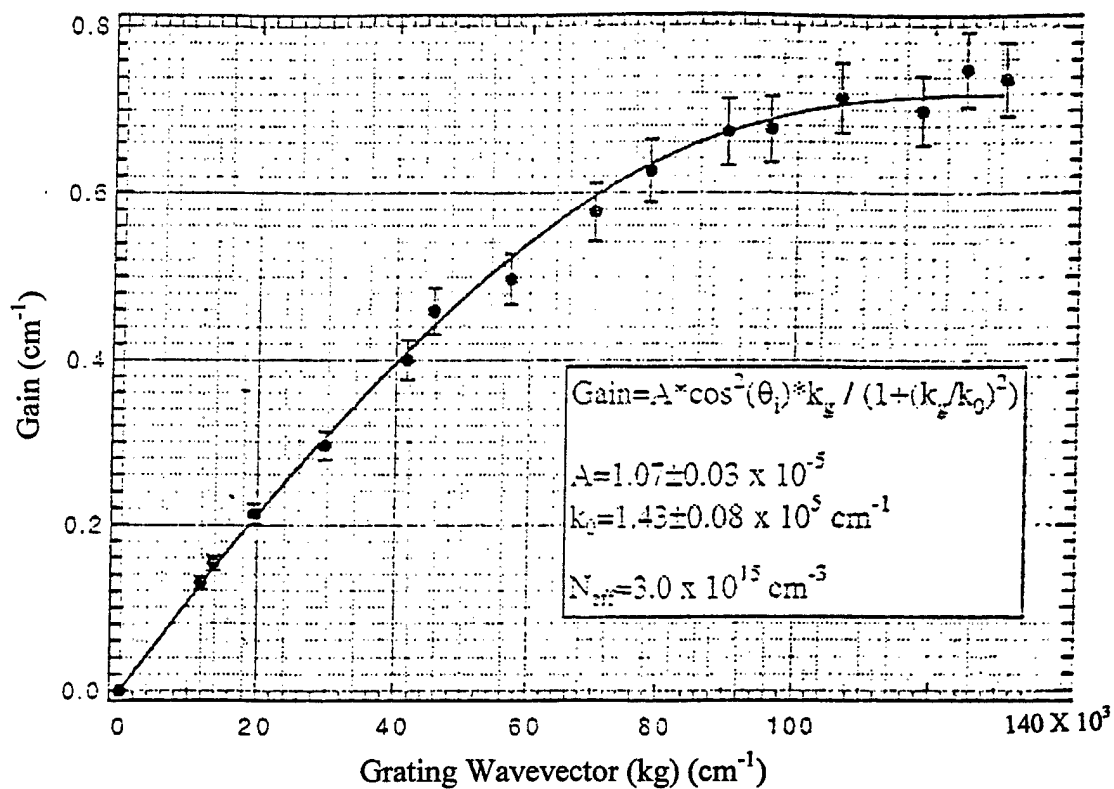

Figure 18. View of the bulk of a ZnTe:V crystal showing significant scattering.

Photorefractive Coupling in ZnTe:V (ZnTe 6/97)
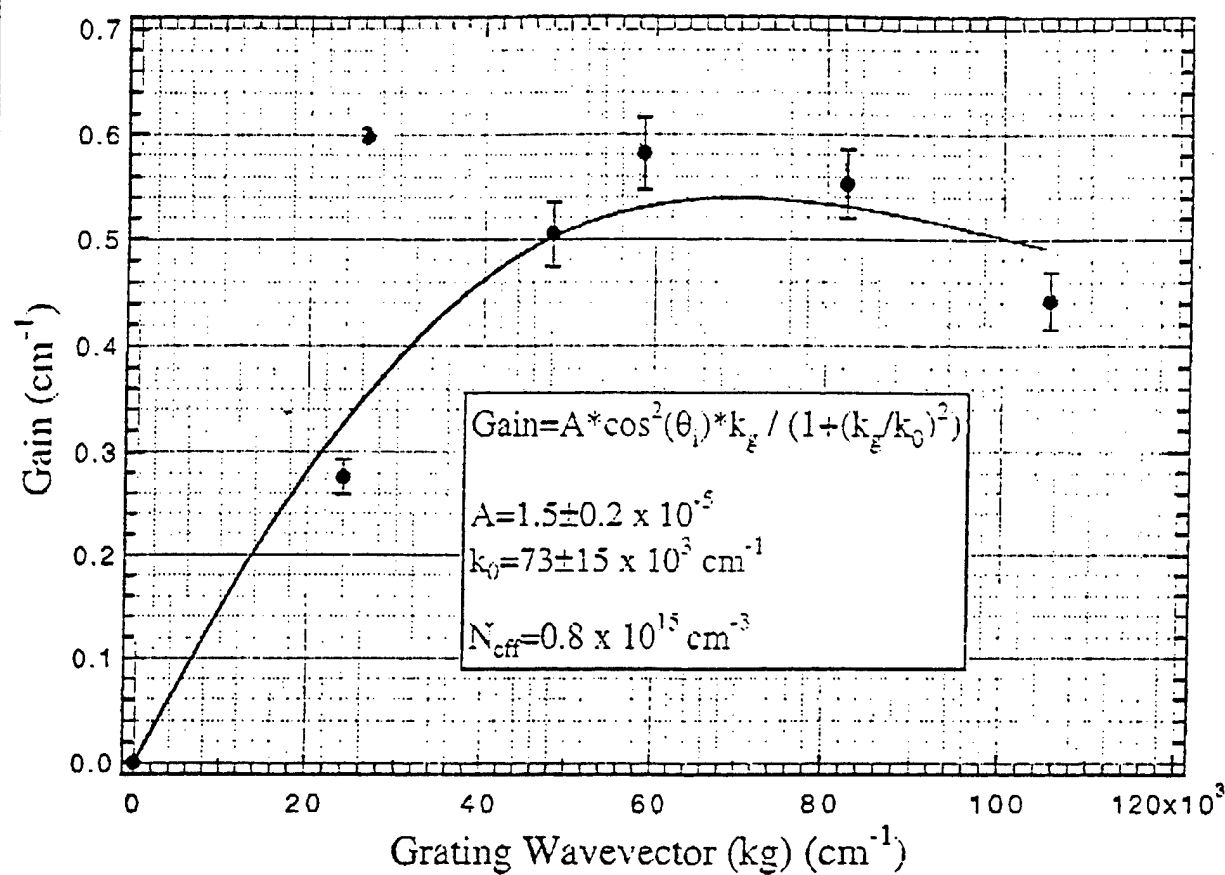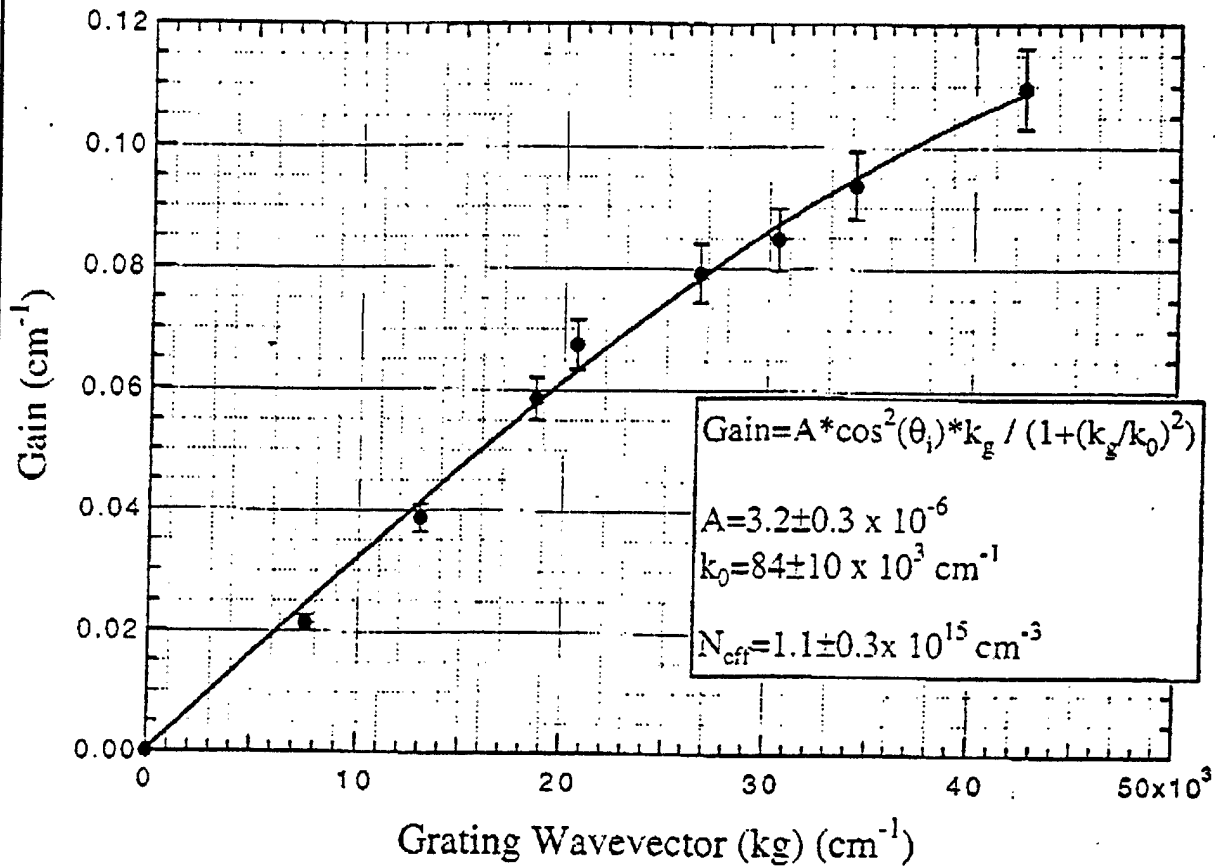
$Gain = A*cos^2(\theta_i)*k_g / (1+(k_g/k_0)^2)$

$A = 1.07 \pm 0.03 \times 10^{-5}$

$k_0 = 1.43 \pm 0.08 \times 10^5 \ cm^{-1}$

$N_{eff} = 3.0 \times 10^{15} \ cm^{-3}$

Wavelength = 775nm

Intensity = 6W/cm^2

Figure 19   Photorefractive coupling in ZnTe:V at $\lambda = 775$ nm.

Figure 20　　　**Photorefractive coupling in ZnTe:V at $\lambda = 860$nm.**

Figure 21   Photorefractive coupling in ZnTe:V at λ = 1064nm.

Results of the photorefractive measurements from another ZnTe:V crystal are shown in Figure 22. This figure shows the photorefractive gain versus the grating wavevector measured using a source wavelength of 780 nm and an intensity of 2.5 W/cm^2. The grating was along the <111> direction and the polarization was parallel to k_g. The solid line in the plot corresponds to k_o =
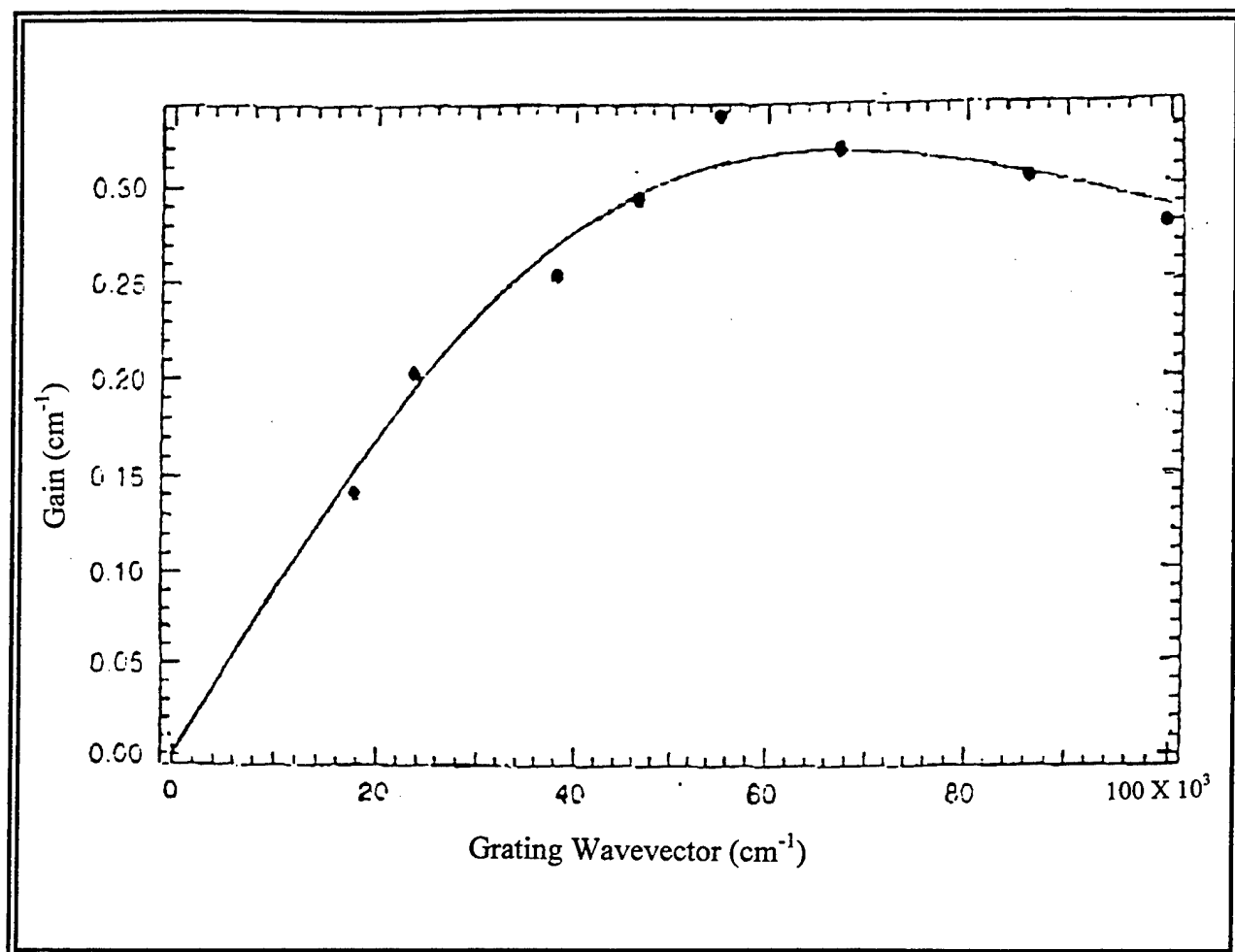
Figure 22   Photorefractive coupling in ZnTe:V at λ = 780nm.

The two-beam coupling gain versus grating period for the wavelengths 0.75μm, 1.06μm and 1.3μm for a co-doped ZnTe (ZnTe:V:Mn) sample are shown in Figure 23. This sample of ZnTe was photorefractive from < 700nm to at least 1.3μm. There is no sign of gain reversal due to electron-hole competition, and the drop in gain with wavelength is as expected. The effective electro-optic coefficient determined by fitting the data to the theory is 2.4 pm/V, which is somewhat less than expected for ZnTe.
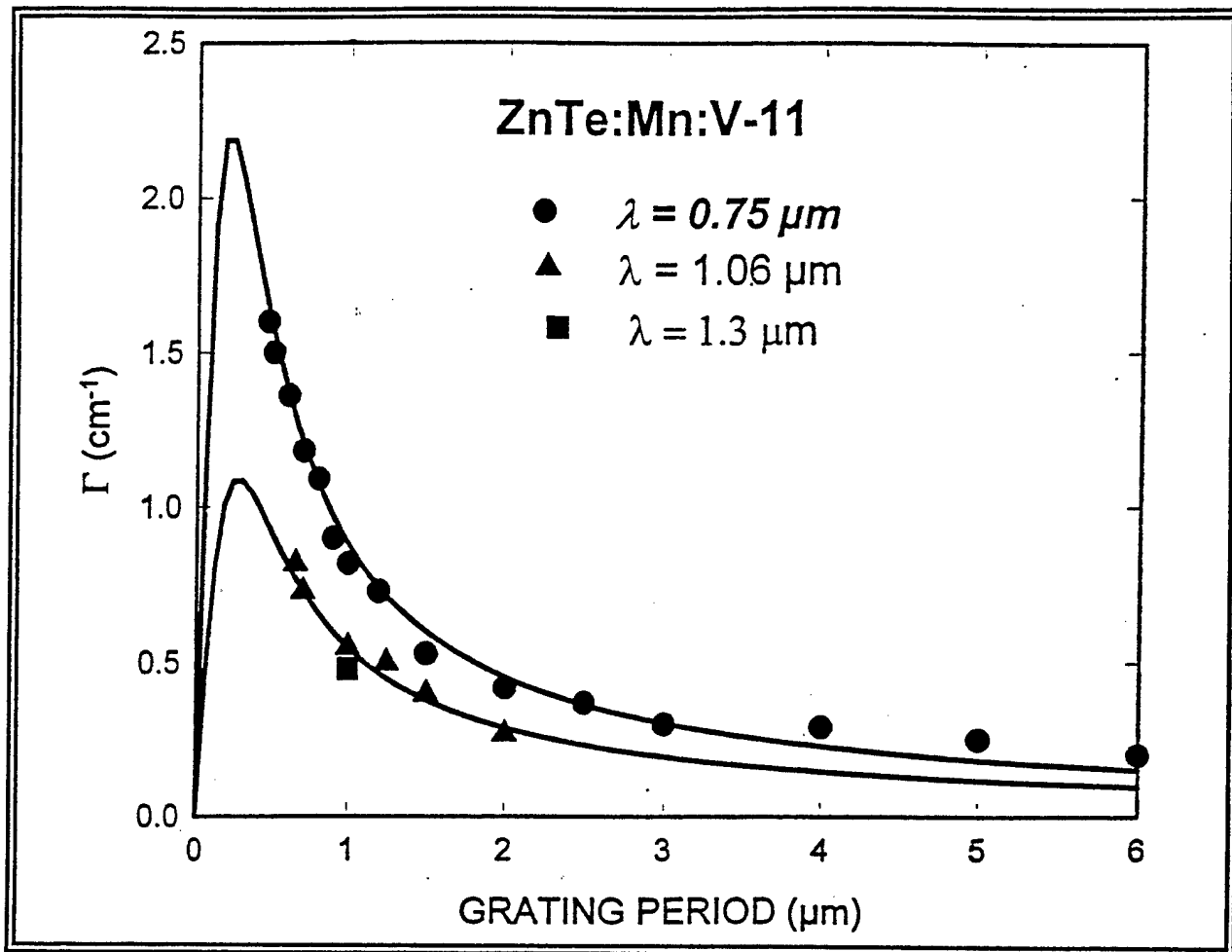
Figure 23   Two beam coupling gain versus grating period at different wavelengths
for ZnTe:Mn:V.

Figure 24 shows the two-beam coupling gain as a function of intensity. There is no fall off in gain due to dark current down to intensities of 0.1 mW/cm^2.
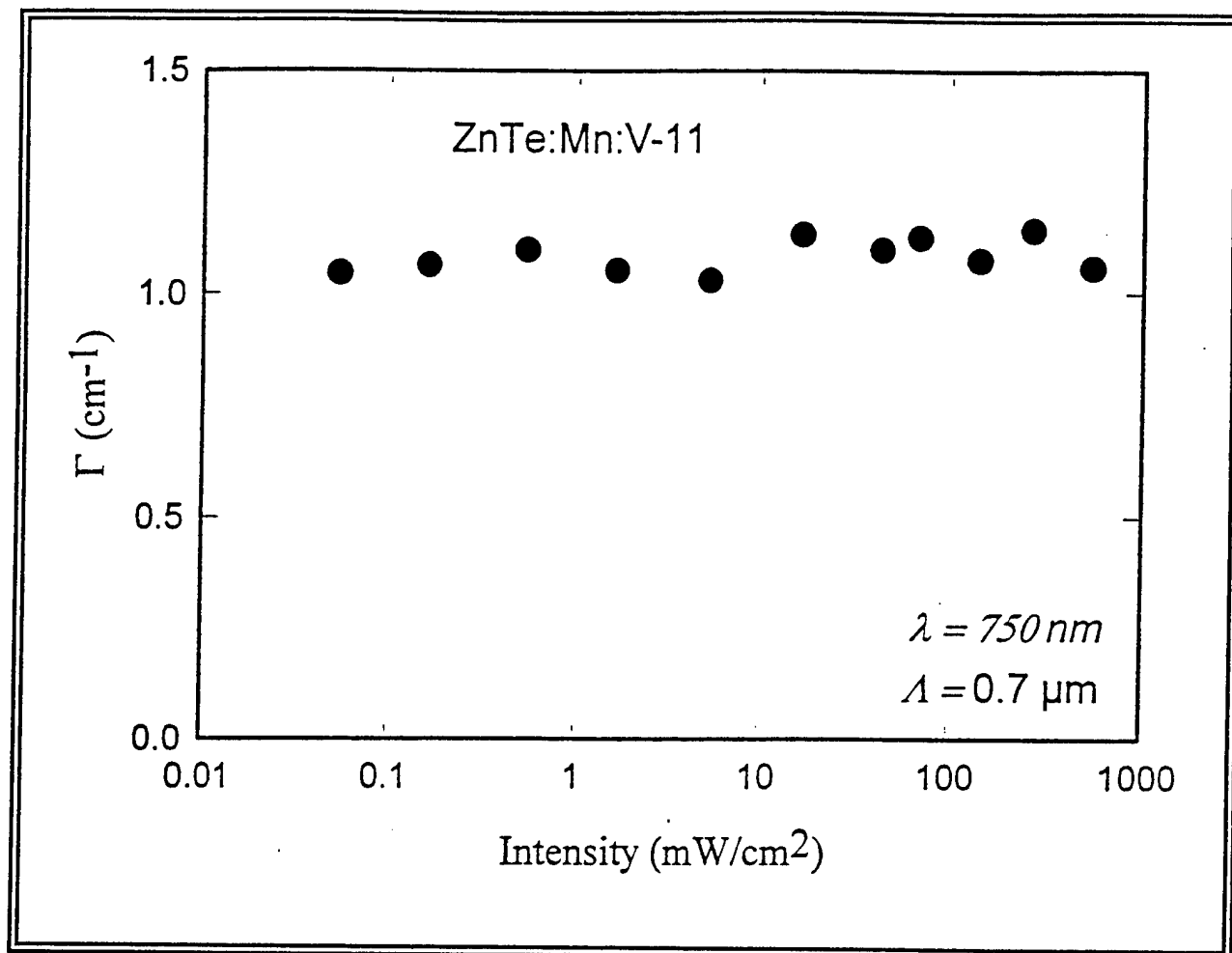
Figure 24   Two beam coupling gain as a function of intensity for ZnTe:Mn:V.

Finally, Figure 25 shows the photorefractive response time versus intensity. The slope of the line is -0.95, which is very close to Γ^1 dependence, indicating that secondary centers are not present, or at least do not contribute to the photorefractive effect at these intensity levels.
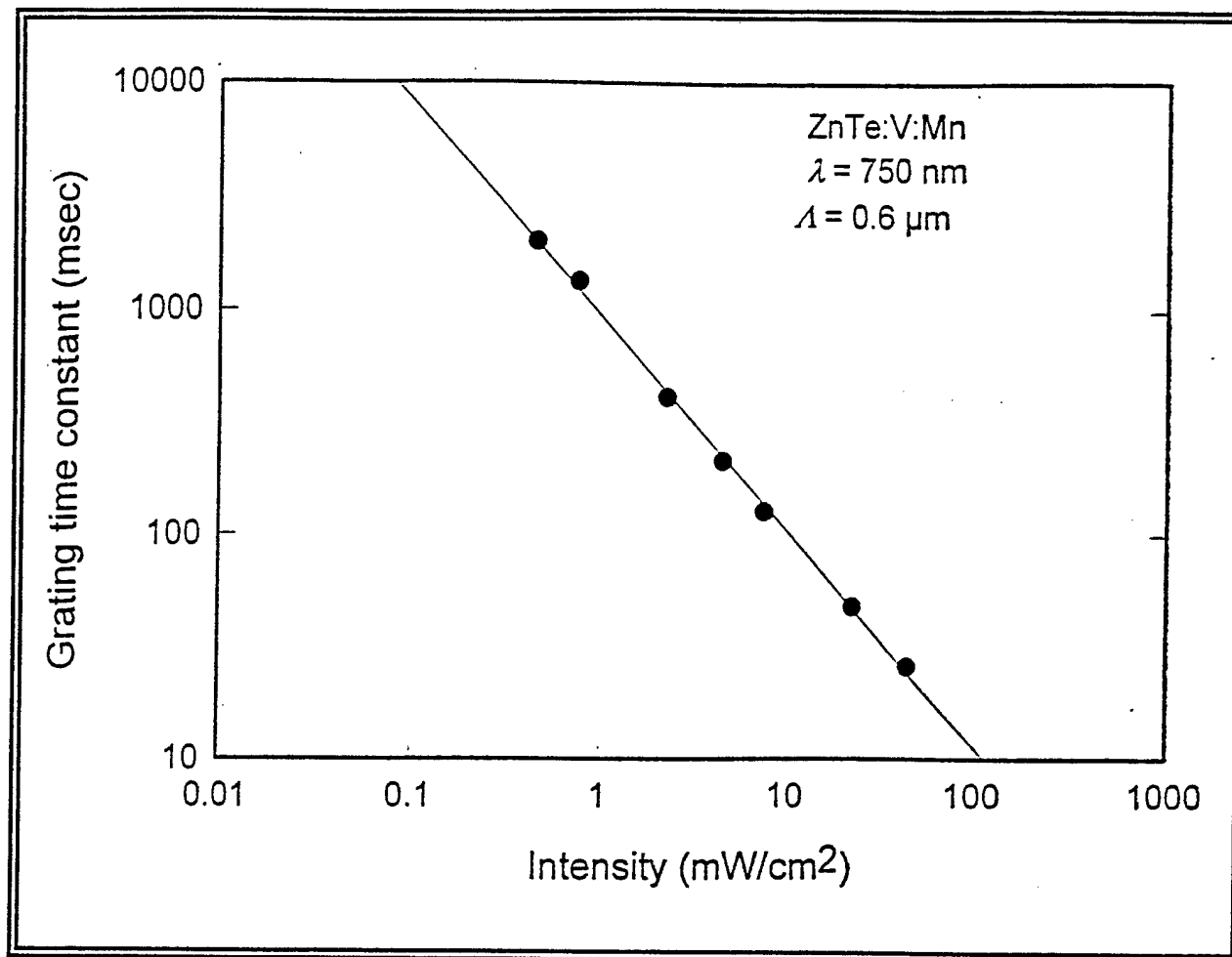
Figure 25   **Photorefractive response time versus intensity for ZnTe:Mn:V.**

We also characterized the transmission and photorefractive coupling of the scandium doped ZnTe sample. The absorption curves and transmission spectrum for this sample are shown in Figure 26. The transmission in the NIR was approximately 80% after correction for Fresnel reflection. Figure 27 shows the photorefractive gain (Γ) versus the grating wave vector (k_g) for this same sample. This crystal of ZnTe:Sc had an optimal grating spacing of 1.6 μm at λ = 776 nm.
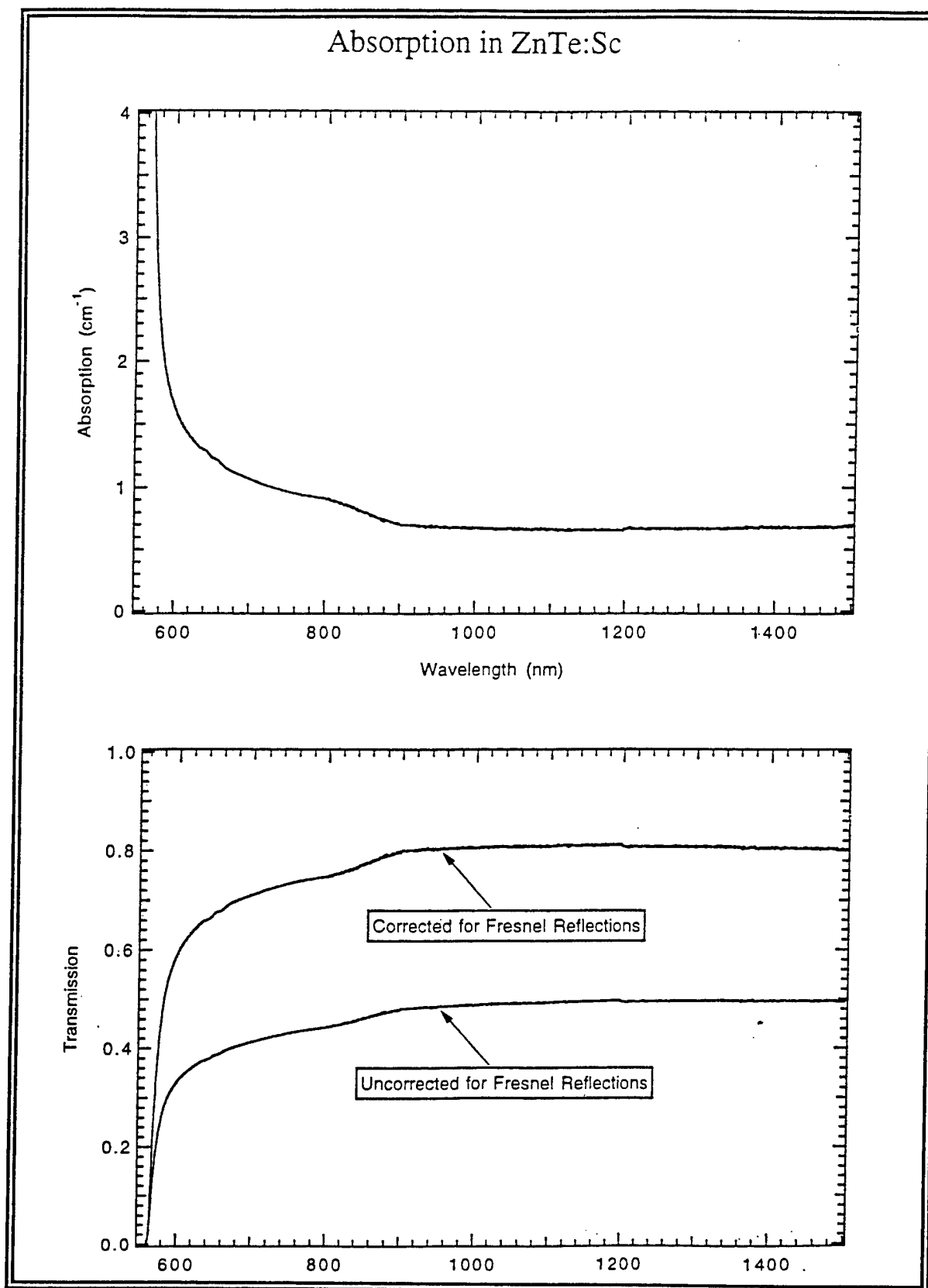
Figure 26 Absorption curves and transmission spectrum for ZnTe:Sc.
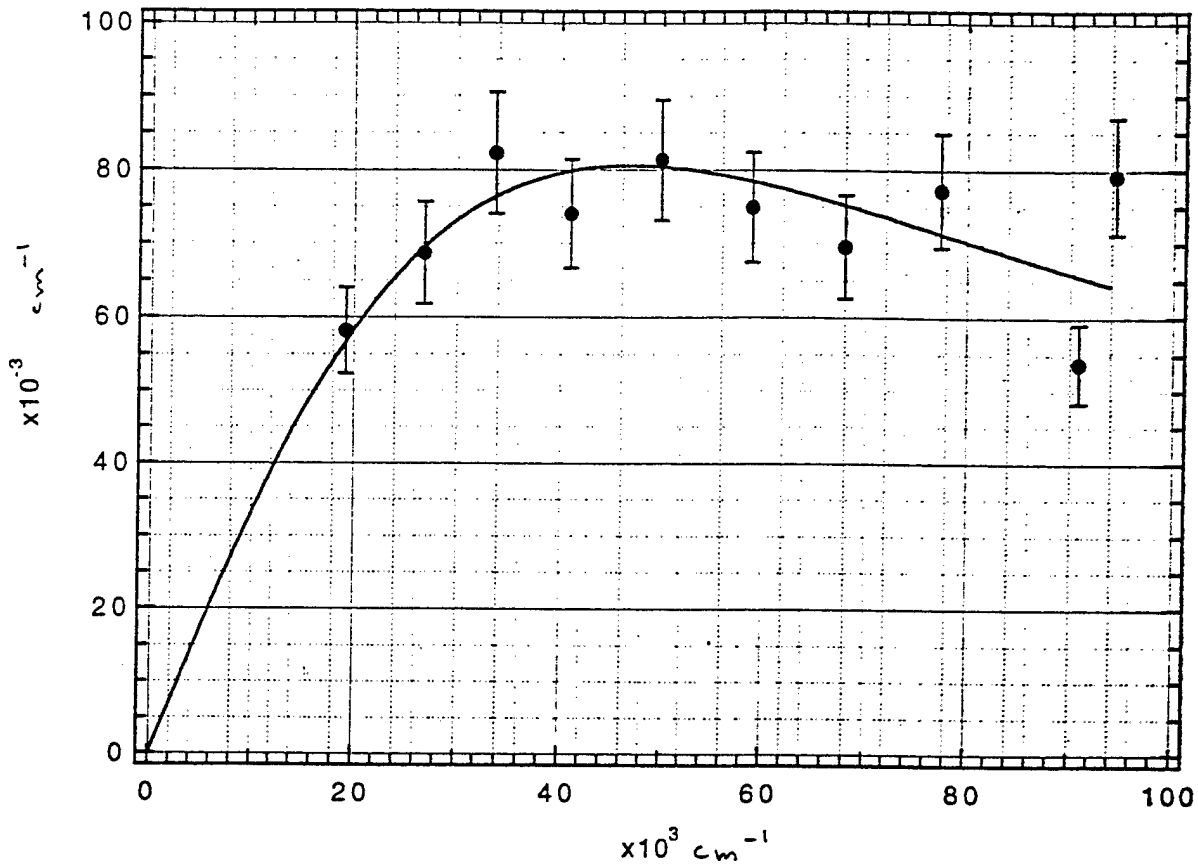
Figure 27   Photorefractive coupling for ZnTe:Sc at $\lambda = 776$nm.

4.3   Characterization of $Cd_{1-x}Zn_xTe$

Because of the separation between the liquidus and solidus curves in the pseudobinary phase diagram of CdTe-ZnTe [13], growth of high quality $Cd_{1-x}Zn_xTe$ is difficult to achieve. This phase separation leads to segregation between the components and poor compositional

homogeneity in the as-grown crystal which in turn lead to increased scattering and variation in wavelength response. Consequently, most of the $Cd_{1-x}Zn_xTe$ crystals (approximately 90%) that were grown during this project had no transmission in the near infrared wavelength region. Furthermore, those crystals which were transparent in the NIR had fairly high absorption. During this project, we were able to grow one $Cd_{1-x}Zn_xTe$ crystal with relatively low absorption in the NIR. This crystal had a 10% composition of zinc (ie, $Cd_{0.90}Zn_{0.10}Te$). The absorption curve for this crystal is shown in Figure 28. This crystal showed a minimum in absorption near the 1.3 μm range. At 1.318 μm, the absorption coefficient was α=0.289 cm^{-1}. Photorefractive measurements performed at 1.3 μm and at a grating spacing of 1 μm showed the gain to be $\sim$ 0.27 cm^{-1}.
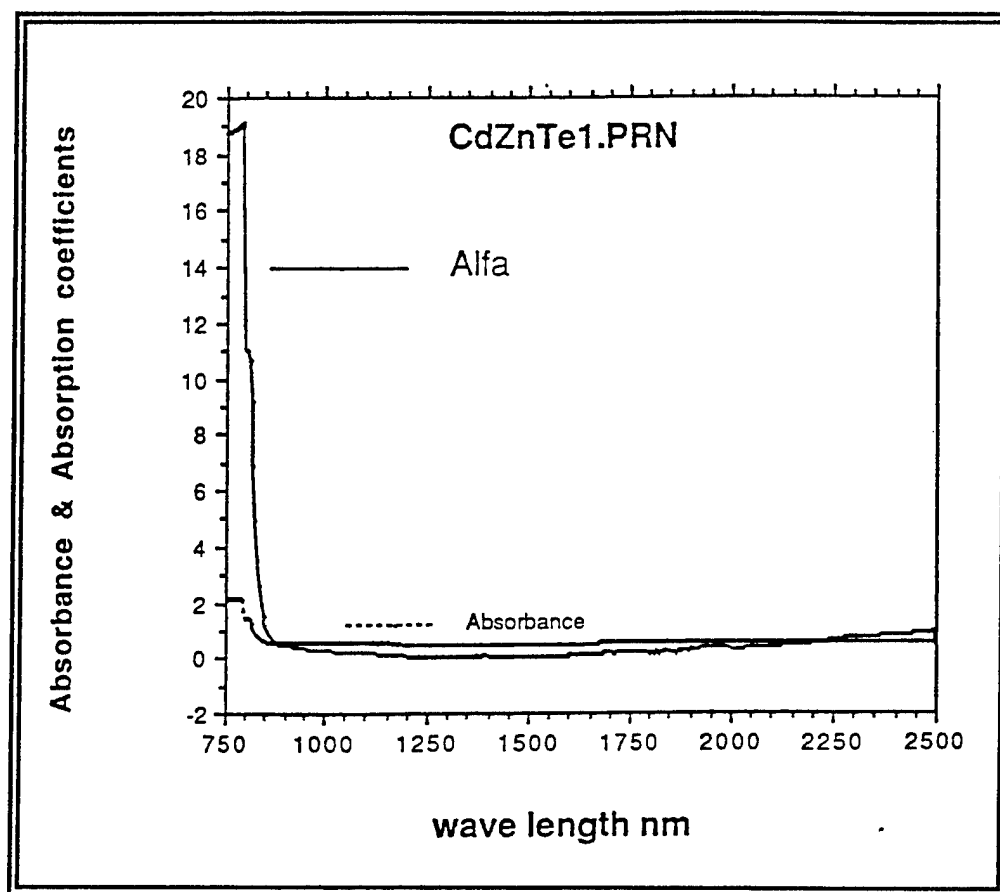
Figure 28   **The absorption curve for $Cd_{0.90}Zn_{0.10}Te$ crystal.**

In order to achieve device quality $Cd_{1-x}Zn_xTe$ crystals, it is necessary to reduce the segregation of the components during growth. One way that this can be achieved is to grow the crystals using the travelling heater method (THM). THM involves the slow, relative movement of a tellurium zone through a source material of good compositional uniformity. Typically, high

quality homogeneous material can be obtained through very precise temperature control, high temperature gradients in the growth region, and a low speed of growth. Thus, use of THM with a strict control over the solid/liquid interface during growth should be investigated for the production of photorefractive $Cd_{1-x}Zn_xTe$ crystals.

5.0   Conclusions

In order to attain the goal of this research, the following tasks were performed:

1. Purification of the constituent elements (cadmium, tellurium and zinc) through vacuum distillation and sublimation.
2. Synthesis of the compounds (CdTe and ZnTe).
3. Low super saturation nucleation and "contactless" growth by physical vapor transport of ZnTe and CdTe crystals.
4. Bridgman growth of CdTe and $Cd_{1-x}Zn_xTe$ crystals.
5. Investigation of growth rate as a function of furnace profile, ampoule geometry, material stoichiometry and hydrogen pressure.
6. Sample preparation and orientation using x-ray diffraction and Laue analysis.
7. Examination of the internal crystalline structure of the grown crystals using infrared and visible microscopy.
8. Characterization of the crystals in terms of their transport properties and optical transmission.
9. Photorefractive characterization of the crystals.
10. Optimization of growth conditions based on crystal analysis.

In this work, we demonstrated the growth of ZnTe and CdTe crystals using a modified "contactless" method in which nucleation occurs at low supersaturation. Nucleation at low supersaturation provides a nucleus with very good crystallographic qualities and the resulting crystals were high quality. Crystals 24mm in diameter and up to 40gm in weight were grown in specially designed ampoules. These ampoules were constructed in such a way that additional purification and improvement of stoichiometry of the source material during growth was possible. Vanadium and manganese doping at a level sufficient to produce photorefractive material was achieved.

We found during our work that only the transition metal vanadium was successful in producing photorefractivity when used as the dopant in the CdTe and $Cd_{1-x}Zn_xTe$ crystals. The addition of manganese along with the vanadium was found to enhance the photorefractive properties of the crystals, but manganese alone did not induce photorefractivity in the crystals. We also found that the transition metal scandium produced photorefractive material when added to ZnTe, so during this project, one scandium doped ZnTe crystal was grown. At this time, the role of the vandium dopant in the band structure of the photorefractive crystals is not clearly understood. Thus, further study into this area is needed in order to optimize the photorefractive gain of these crystals.

During this work we also grew crystals of CdTe and $Cd_{1-x}Zn_xTe$ crystals using the Bridgman technique. Because of the separation between the liquidus and solidus curves in the pseudobinary phase diagram, growth of high quality $Cd_{1-x}Zn_xTe$ is difficult to achieve. Consequently, most of the $Cd_{1-x}Zn_xTe$ crystals that were grown during this project had no transmission in the near infrared wavelength region. Furthermore, those crystals which were transparent in the NIR had fairly high absorption. During this project, we were able to grow one $Cd_{1-x}Zn_xTe$ crystal with relatively low absorption in the NIR, and this crystal did exhibit photorefractivity with a gain of approximately $0.22cm^{-1}$ at $\Lambda_g = 1.3\mu m$ and $\lambda = 1.3$ μm. Further investigation into the growth of photorefractive $Cd_{1-x}Zn_xTe$ is warranted.

The crystals grown during this project were evaluated based on optical, electrical and structural characterization. The photorefractive measurements conducted during this work were carried out at $0.633\mu m$, the semiconductor laser wavelength range of 0.700 to $0.850\mu m$ and the important optical communication wavelengths of 1.3 and $1.5\mu m$. In vanadium doped ZnTe, we observed a photorefractive gain of $0.6cm^{-1}$ at a wavelength of $0.80\mu m$ and a grating spacing of $1\mu m$. The photorefractive gain observed in vanadium-manganese codoped ZnTe was much higher than the gain in ZnTe:V. The photorefractive gain in ZnTe:V:Mn (at $1\mu m$ grating spacing) at $0.63\mu m$ was $1.52cm^{-1}$ and at $0.80\mu m$ it was $1.3cm^{-1}$. In CdTe:V, the two beam coupling gain at $\Lambda_g = 0.6\mu m$ and $\lambda = 870nm$ was approximately 1.1 to 1.2 cm^{-1}.

With the successful growth of high quality crystals, our materials can be used in a variety of applications involving detectors and electro-optic devices.

36

6.0 References

[1] A. Partovi, J. Millerd, E.M.Garmire, M.Ziari, W.H.Steier, S.B.Trivedi and M.B.Klein. *Appl. Phys. Lett.* **57**, 846 (1990).

[2] M. Ziari, W.H. Steier, P.N. Ranon, M.B. Klein and S.B. Trivedi. *J. Opt. Soc. Am. B.* 1461-1466 (1992).

[3] R.N. Schwartz, M. Ziari and S.B. Trivedi. *Phys. Rev. B*, **49**, 5274 (1994).

[4] M. Ziari, W.H. Steier, P.N. Ranon, M.B. Klein and S.B. Trivedi. paper presented at the *Annual Meeting of the Optical Society of America*, Nov. 3-8, 1991, San Jose, CA.

[5] H.J. Von Bradleben et al, "Defects in photorefractive CdTe:V and electron paramagnetic study," *Applied Physics Letters* **63** 8 (1993) 1140.

[6] K.Grasza, J.Cryst.Growth 146(1995) 65.

[7] K.Grasza, S.B.Trivedi, Zengchen Yu, S.W.Kutcher, W.Palosz, G.A.Brost, "Low supersaturation nucleation and 'contactless' growth of photorefractive ZnTe crystals", J.Crystal Growth 174 (1997) 719-725.

[8] K.Grasza, S.B.Trivedi, Zengchen Yu, S.W.Kutcher, G.A.Brost, J. Crystal Growth 174 (1997) 263-266.

[9] Knacke, O. Kubaschewski, K. Hesselmann, "Thermochemical Properties of Inorganic Substances", Springer Verlag, 1991.

[10] K.Grasza, "Mass and heat transfer in crystal growth",in:"Elementary crystal growth", ed.K.Sangwal, SAAN Publisher, Lublin 1994.

[11] O.Knacke,O.Kubaschewski,K.Hesselmann, "Thermochemical Properties of Inorganic Substances", Springer-Verlag, 1991.

[12] K.Grasza and A.Jedrzejczak, "Growth stability in the high   temperature vapor growth", J.Crystal Growth, 162 (1996) 173.

[13] Jacques Steininger, Alan J. Strauss, and Robert F. Brebrick. "Phase diagram of the Zn-Cd-Te ternary system", J. Electrochem Soc.: Solid State Science, Vol. 117, No. 10 (1970) 1305.